Journal of Applied Research and Technology

www.jart.icat.unam.mx

Journal of Applied Research and Technology 21 (2023) 665-687

Original

Backstepping-ANFIS hybrid controller design for cooperative quadrotors

Mohamed Mahfouz[a]* • Ahmed T. Hafez[b] • Mahmoud M. Ashry[b] • Gamal Elnashar[b]

[a]*Egyptian Armed Forces, Cairo, Egypt*
[b]*Military Technical College, Cairo, Egypt*

Received 08 06 2021; accepted 06 23 2022
Available 08 31 2023

Abstract: This paper offers a novel hybrid control approach for solving the formation problem for a group of cooperative quadrotors unmanned aerial vehicles (UAVs). Two-loop controller layout techniques are presented: one is a backstepping-based PID controller as a higher-controller in external-loop to manage the proportional position orders and create body-axis rate orders for the internal loop. Second, it is an adaptive neuro fuzzy inference system (ANFIS). Controller acts as a lower-controller in the internal-loop to generate desired angular rotations for every quadrotor, separately. The introduced hybrid controller is applied to overcome the formation aviation downside that keeps track of the leader-follower approach. The main contribution in this work lays in solving the formation problem for a team of cooperative quadrotors through hybrid backstepping and ANFIS controller in a free and loaded obstacle environment. A complete model of six-degree of freedom for a group of cooperative UAVs is used in the MATLAB Simulink to perform various simulations to validate the hybrid proposed controller. Simulation results for a team of cooperative UAVs show the success of the proposed approach in solving the formation configuration problem for the UAV team members.

Keywords: Quadrotor, UAV, backstepping, ANFIS

*Corresponding author.
E-mail address: m.mahfouz.trc@gmail.com(Mohamed Mahfouz).
Peer Review under the responsibility of Universidad Nacional Autónoma de México.

1. Introduction

Unmanned air vehicle (UAV) which is further known as unmanned aircraft system (UAS) has reached a unique grades of evolution in military and civilian implementations (Ashry, 2019; Hou et al., 2017). UAVs are capable of executing hazard missions with zero risk for human pilots (Madani & Benallegue, 2006) and distinguished with their ease of deployment, high-motility, and low maintenance value (Shakhatreh et al., 2018). These characteristics open the door to researchers for new ranges in aerospace fields, where it allows using UAS in several assignments like forest meteorology (Gallay et al., 2016), environmental observance (Alfeo et al., 2018), temperature variation (Liu et al., 2018), ice rivers dynamics (Ryan et al., 2017), volcanic activities (Mori et al., 2016; Nakano et al., 2014), atmospheric sampling (Greatwood et al., 2017; Techy et al., 2010), border inspection patrol (Gupte et al., 2012; Ghazbi et al., 2016), traffic regulation (Elloumi et al., 2018), discrimination and surveillance vehicles (Finn & Wright, 2012; Li et al., 2008), seeking-and-relief operations (Shakernia et al., 1999).

UAVs are classified into different types according to their structure, one of the most demanded UAV structure nowadays is the rotor vertical take-off and landing (VTOL) craft referred to as quadrotor (Ghazbi et al., 2016). It can be sorted as a rotating wing VTOL airliner due to its ability for vertical takeoff and landing, flight forward, and hover at a desired location (Martinez, 2007). Compared with other types of UAVs, and by its singular features, quadrotor took the advantage to print its distinctive stamp in aircraft systems (Raymer, 2006; Zhang et al., 2014). Quadrotor is characterized by its ease of design, control simplicity, high maneuverability, small size, convenient payload capacity, silent operations, and high maneuver elasticity (Gupte et al., 2012; Kivrak, 2006; Li et al., 2015). These attributes enable using quadrotors in vital applications such as seeking-and-relief tasks in difficult and dangerous areas beside rapid intervention assignments (Gharibi et al., 2016; Ghazbi et al., 2016). The researchers were motivated to develop quadrotors control systems with the attraction of its simplicity. The simple shape of four mounted rotors symmetrically on equal perpendicular axis allow the designers to control quadrotor by adjusting the speed of each rotor (Ghazbi et al., 2016; Rahman et al., 2016). Both attitude channels and linear velocity can be controlled through rotor speed (Bouabdallah & Siegwart, 2007). This control approach is successfully applied in utilizing small quadrotors worked using electric motors. In this case, the mechanical complexity of the rotor is decreased (Özbek et al., 2015), and different control techniques can be applied on the electric motors for semi-autonomous and full autonomous flight (Zulu & John, 2016).

Due to modern tasks complexity and expansion nature of most targeted fields, the researchers start to use cooperative multiple quadrotors in performing most of the new missions. This is known as swarm system (Jia et al., 2018). The swarm system is inspired initially by observing biological phenomena. Observation results confirmed the fact that competence and performance can be enhanced, if biological creatures work together in a group (Zhu et al., 2016). Multiple quadrotor swarm VTOL systems consist of at least couple of simple autonomous quadrotors working together to accomplish specific demanded mission (Ekawati et al., 2016). This swarm of multiple cooperative quadrotors can work composing a certain geometric shape called formation (Wu et al., 2017; Yang, Ji et al., 2017). The formation architectures are divide into a pre-designed formation and adaptively architectures (Oh et al., 2017). According to the type of the formation, the cooperation between the team members is realized depending on the behavior of each quadrotor which takes into its consideration the behavior of the other group members in both free and in obstacle-loaded air domain (Farinelli et al., 2004). This interaction, communication, and exchange information are essential to achieve an overall group operation (Zhang & Mehrjerdi, 2013).

Swarming algorithms were inspired by the natural phenomena of animal cooperative aggregate motions (Reynolds, 1987).

Swarming or grouping behaviors can be openly seen in droves of birds, colonies of ants, schools of fish, and flocks of animals (Okubo, 1986; Parrish et al., 2002). Swarming becomes a field of interest for the researchers in the field of cooperative UAVs (Ashry et al., 2008). Swarming algorithms are varied between classical algorithms and intelligence algorithms (Yang, Wang et al., 2017). For instant, simple classical intelligence swarming algorithms were used to solve the swarming problem in affected by the behavior of ants where an optimized solution was introduced to solve the swarming problem (Colorni et al., 1991; Eberhart & Kennedy, 1995).

In the last decade, several advanced intelligent swarming approaches were presented to tackle the swarming problem (Abbass, 2001; Eusuff & Lansey, 2003; Karaboga, 2005; Pan, 2011; Sun et al., 2014; Wu et al., 2013; Yang, 2010a; 2010b; 2012; Yang & Deb, 2009). Several control techniques were used to solve the swarming problem for a cooperative UAVs team. One of the new valuable control approaches in the field of UAVs is the combination of backstepping and ANFIS controllers. This combination has been executed in the control of numerous sorts of non-linear systems. In (Khari et al., 2015), a generalized backstepping approach combined with an ANFIS approach was applied to control a nonlinear Lorenz chaotic system. This introduced approach guarantees that the generalized backstepping approach achieves its optimal parameter using ANFIS. In Asad et al. (2017), an MEMS gyroscope was controlled by a backstepping sliding approach based on type-2 fuzzy controller.

Moreover, the altitude stabilization of a hypersonic missile was controlled using a combination of backstepping and ANFIS controllers (Allahverdy & Fakharian, 2019).

On one hand, the backstepping approach was used in the analysis of the missile altitude dynamics. On the other hand, the ANFIS approach was applied to calculate the uncertainty model parameters. In (Azar et al., 2020), the stabilization of a dynamic framework of port-Hamiltonian systems is controlled by a combination of backstepping and ANFIS controllers. Also, ANFIS was utilized to estimate the ordinary backstepping sliding mode control law to enhance the performance of a non-linear system in (Tavoosi, 2020).

Most backstepping control strategies are utilized as an upper hand controller (Fethalla et al., 2017; Rego et al., 2016; Vallejo-Alarcón et al., 2015). Backstepping controller is an effective control strategy for extremely nonlinear frameworks (Basri et al., 2015; Lee et al., 2017; Liu et al., 2015; Mutawe et al., 2021).

The rapid convergence rate, the stability, the capability to manage nonlinear frameworks using recursive operation of Lyapunov function, the robustness regardless presence of uncertainties, and the simplicity are the benefits of backstepping controller (Madani & Benallegue, 2006).

Similarly, ANFIS controller is a moderate artificial intelligent control technique. It integrated the power of fuzzy logic (FL) approaches parallel processing and intelligent learning capacities of expert artificial neural networks (ANN). In its essence, ANFIS incorporates the benefits of the ANN and FL, and erases the drawbacks of the ANN and FL as well (Premkumar & Manikandan, 2018).

In this paper, the benefits of backstepping and ANFIS are combined in the proposed approach which leads to improve the overall performance and robustness in the presence of disturbances and noise.

The main contribution of this paper lays in solving the problem of cooperative UAVs formation using a cascaded backstepping and ANFIS controller. This hybrid controller combines the backstepping-based PID controller with the ANFIS controller.

A proposed aggregate controller depending on the position controller is introduced to regulate the translational dynamics of cooperative UAV group to pursue the pre-planned formation path. Moreover, an attitude controller is designed to keep stability of the inner rotational dynamics.

This paper is organized as follows:

Section 2 introduces briefly the underlying quadrotor mathematical paradigm, and the hybrid controller design is demonstrated in Section 3. In Section 4, the simulation results for a group of cooperative quadrotors following a desired trajectory path using the designed hybrid controller are presented. The stability analysis of the proposed controller is discussed in Section 5, while in Section 6 a discussion about the underlying hybrid controller results is introduced. Finally, conclusion and future work are introduced in section 7.

2. Quadrotor schematic model

The underlying quadrotors are distinguished by a uniformed schematic. Each quadrotor consists of four rotors mounted at proportional distance from the center point and the rotors are set to provide necessary effort to all sort of quadrotor movements.

The quadrotor controller is accomplished by changing the speed of every rotor of the fourfold rotors (Mahfouz et al., 2018). A voltage applied on every motor cause a net torque being utilized on the rotor shaft producing a thrust force T_i for i_{th} quadrotor and j_{th} rotor, where $j = 1, 2, 3, 4.$ Once the rotor blade is spinning, there is a proportional speed difference among the rotor sharp edge and air during rotating clockwise and anti-clockwise causing a net moment around the roll hub. Further speed also creates a power drag on the rotor which is opposed to travel orientation D_i , the thrust is realized through aerodynamic coefficients C_{Ti} as in (1) (Azzam & Wang, 2010):

$$T_i = \frac{1}{2} C_{Ti} \rho_i A_i \Omega_i^2 R_i^2 \tag{1}$$

where ρ_i is the air density, A_i represents the area of the blade, Ω_i performs the propeller's angular velocity, and R_i states the radius of the blade.

A group of fourfold control inputs parameters η_i are acquired like a function of normalized singular thrust and torques as in equations (2-4).

At hovering and semi hovering states when nonlinear components can be neglected as in (Mahfouz et al., 2019), the thrust and forces are corresponding to the square of propellers' spinning speed. The thrust and drag forces can be calculated by Azzam and Wang (2010), Mahfouz et al. (2013):

$$T_i = \beta_T \Omega_i^2 \tag{2}$$

$$D_i = \beta_D \Omega_i^2 \tag{3}$$

where β_T , and β_D are constants. The thrust, rolling, pitching, and yawing moments are obtained in (4) (Mahfouz et al., 2013):

$$\begin{cases} \eta_{1i} = \beta_{Ti} \sum_{j=1}^{4} \Omega_{ji}^2 \\ \eta_{2i} = \beta_{Ti} (\Omega_{1i}^2 - \Omega_{3i}^2) \\ \eta_{3i} = \beta_{Ti} (\Omega_{2i}^2 - \Omega_{4i}^2) \\ \eta_{4i} = \beta_{Di} (\Omega_{2i}^2 + \Omega_{4i}^2 - \Omega_{1i}^2 - \Omega_{3i}^2) \end{cases} \quad (4)$$

In modeling strategy of the VTOL quadrotor, the rotational transmutations aren't performed within the identical formation to relocate from the earth to the body coordinate.

Naturally, the ultimate efficient technique performs the resultant rotation of the earth to the body transmutation over the thrust side. Assume a steady-earth coordinate E and a steady-body coordinate B. Utilizing Euler angles specifications; the air-coordinate direction in space is defined by a rotation matrix R. So, for the body to the earth transmutation, R is counted in (5) (Ashry, 2014; Mahfouz et al., 2013):

$$R_{xyzi} = \begin{bmatrix} s\theta_i s\phi_i s\psi_i + c\psi_i c\theta_i & s\phi_i s\theta_i c\psi_i - c\theta_i s\psi_i & s\theta_i c\phi_i \\ c\phi_i s\psi_i & c\psi_i c\phi_i & -s\phi_i \\ c\theta_i s\psi_i s\phi_i - s\theta_i c\psi_i & c\theta_i s\phi_i c\psi_i + s\theta_i s\psi_i & c\theta_i c\phi_i \end{bmatrix} \quad (5)$$

where: ϕ_i, θ_i, ψ_i roll, pitch, and yaw angles for the i_{th} quadrotor, respectively; $s \equiv \sin, \quad c \equiv \cos.$

The evolution of a convenient attitude controller for the quadrotor targeted a precise active model to be progressed. Newton laws were chosen to estimate the quadrotor dynamics for the simplicity of the control goals.

The Newtonian approach is a definitive proper option for designing robust frameworks in 6-degree-of-freedom (Bang et al., 2004). The Newtonian hypothesis exercised in order to produce a robust framework in 6DOF are well represented in (Hamel et al., 2002; Tayebi & McGilvray, 2006).

Assuming the dynamics of a robust framework underneath forces F_i^b, and moments τ_i^b. These parameters are used at the middle point of mass and stated in the steady-body coordinate. It is represented in Newton-Euler approach as follows (Mahfouz et al., 2019; Murray et al., 1994):

$$\begin{cases} F_i^b = m_i \dot{v}_i^b + \omega_i^b \times m_i v_i^b \\ \tau_i^b = I_i \dot{\omega}_i^b + \omega_i^b \times I_i \omega_i^b \end{cases} \quad (6)$$

where m represents the quadrotor overall body mass, v_i^b performs the speed vector in the steady-body coordinate, ω_i^b states the angular velocity at the steady-body coordinate, and I_i symbolizes the body moment of inertia matrix.

The quadrotor equations of motions are introduced in (7) (Bouabdallah, 2007; Bouabdallah & Siegwart, 2007; Mahfouz, 2015; Wierema, 2008):

$$\begin{cases} I_{xxi}\ddot{\phi}_i = \dot{\theta}_i\dot{\psi}_i(I_{yyi} - I_{zzi}) + J_{ri}\dot{\theta}_i\Omega_{ri} + l_i(-T_{2i} + T_{4i}) - h_i\sum_{j=1}^{4} H_{yji} + (-1)^{j+1}\sum_{j=1}^{4} R_{mxji} \\ I_{yyi}\ddot{\theta}_i = \dot{\phi}_i\dot{\psi}_i(I_{zzi} - I_{xxi}) + J_{ri}\dot{\phi}_i\Omega_{ri} + l_i(T_{1i} - T_{3i}) + h_i\sum_{j=1}^{4} H_{xji} + (-1)^{j+1}\sum_{j=1}^{4} R_{myji} \\ I_{zzi}\ddot{\psi}_i = \dot{\phi}_i\dot{\theta}_i(I_{xxi} - I_{yyi}) + J_{ri}\Omega_{ri} + (-1)^{j}\sum_{j=1}^{4} Q_{ji} + l_i(H_{x2i} - H_{x4i}) + l_i(-H_{y1i} + H_{y3i}) \\ m_i\ddot{z}_i = m_i g - (c\phi_i c\psi_i)\sum_{j=1}^{4} T_{ji} \\ m_i\ddot{x}_i = (c\psi_i s\theta_i c\phi_i + s\psi_i s\phi_i)\sum_{j=1}^{4} T_{ji} - \sum_{n=1}^{4} H_{xji} - \frac{1}{2}C_{xi}A_{ci}\rho_i\dot{x}_i|\dot{x}_i| \\ m_i\ddot{y}_i = (s\psi_i s\theta_i c\phi_i - c\psi_i s\phi_i)\sum_{j=1}^{4} T_{ji} - \sum_{j=1}^{4} H_{yji} - \frac{1}{2}C_{yi}A_{ci}\rho_i\dot{y}_i|\dot{y}_i| \end{cases} \quad (7)$$

where $I_{xxi}, I_{yyi}, I_{zzi}$ are body moment of inertia matrices, Q_{ji} is a drag moment, J_{ri} is rotor moment of inertia, H_{xji} and H_{yji} are hub forces.

The proposed hybrid controller consists of position, attitude and altitude controllers.

The position and altitude controllers adjust the motion dynamics in order to track the pre-designed path for the UAV team.

The attitude controller keeps and executes the stability of the inner rotational dynamics.

The introduced control approach in this paper is composed of a two-loop controller layout technique. The outer control loop is a backstepping-based PID controller to trail proportional position orders and create body-axis rate orders for the internal loop.

The inner control loop is an ANFIS controller to generate desired angular rotations for every quadrotor separately, as seen in Figure 1.

One should notice that backstepping-based PID approach is utilized for position and altitude control, while ANFIS approach is used for attitude control.

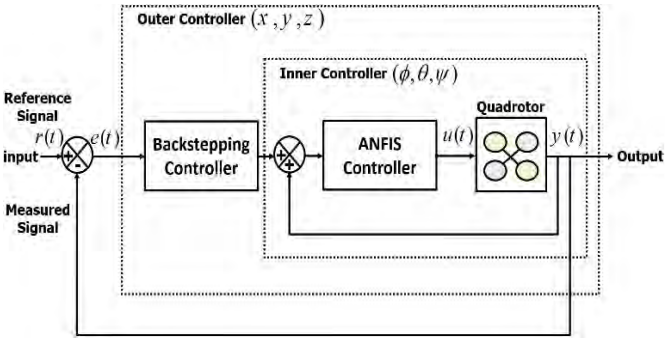

Figure 1. Hybrid controller of backstepping and ANFIS.

The quadrotor control framework is organized in four unique controllers as outlined in Figure 2. VTOL controller yields the required elevation z_d to altitude controller that is based on altitude sensor data to produce the required overall thrust T_d.

Position controller gets quadrotor current location (x, y) and required thrust force. It yields required roll ϕ_d, and pitch θ_d, however, required yaw ψ_d gets through the client directly.

The desired motor speed is produced by the controller after the attitude control is adjusted.

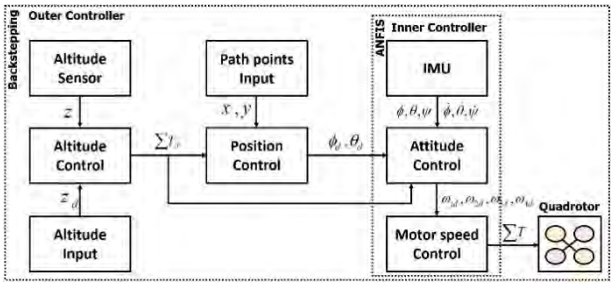

Figure 2. The control architecture of quadrotor.

3. Hybrid control design

3.1. Backstepping-based PID approach

The backstepping-based PID controller is introduced in (Mahfouz et al., 2018). The backstepping control strategy is proposed to achieve the desired altitude and vertical location behavior as a higher-controller in the external-loop. For i_{th} quadrotor, the error in relation in the translation location is the difference between the current and the desired path, and can be defined as:

$$e_i = z_i - z_{di} \tag{8}$$

the first backstepping control error will then be:

$$g_{1i} = k_{1i} e_i + k_{2i} \int e_i dt \tag{9}$$

where k_{1i} and k_{2i} are positive parameters of tuning.

Considering Lyapunov theorem, a positive definite and time derivative negative semidefinite function V_{1i} is proposed as:

$$V_{1i} = \tfrac{1}{2} g_{1i}^2 \tag{10}$$

differentiating (10) will give:

$$\begin{aligned} \dot{V}_{1i} &= g_{1i} \dot{g}_{1i} = g_{1i} (k_{1i} \dot{e}_i + k_{2i} e_i) \\ &= g_{1i} (k_{1i} \dot{z}_i - k_{1i} \dot{z}_{di} + k_{2i} e_i) \end{aligned} \tag{11}$$

where $\dot{z}_i$ is assumed as a virtual control. The proposed virtual control $(\dot{z})_{di}$ can be defined as:

$$(\dot{z})_{di} = \dot{z}_{di} - \frac{k_{2i}}{k_{1i}} e_i - \frac{c_{1i} g_{1i}}{k_{1i}} \tag{12}$$

where $(\dot{z})_{di}$ is negative and c_{1i} is positive in order to raise altitude tracking velocity.

The error in relation to the virtual control $\dot{z}_i$ which represent the rate of the altitude can be defined as:

$$\begin{aligned} g_{2i} &= \dot{z}_i - (\dot{z})_{di} \\ &= \dot{z}_i - \dot{z}_{di} + \frac{k_{2i}}{k_{1i}} e_i + \frac{c_{1i} g_{1i}}{k_{1i}} \end{aligned} \tag{13}$$

the rate of the error $\dot{e}_i$ is defined as:

$$\dot{e}_i = \dot{z}_i - \dot{z}_{di} \tag{14}$$

substituting (14) in (13):

$$g_{2i} = \dot{e}_i + \frac{k_{2i}}{k_{1i}} e_i + \frac{c_{1i} g_{1i}}{k_{1i}} \tag{15}$$

$$\text{so, } g_{2i} = \frac{1}{k_{1i}} (k_{1i} \dot{e}_i + k_{2i} e_i + c_{1i} g_{1i}) \tag{16}$$

differentiating (9) will give:

$$\dot{g}_{1i} = k_{1i}\dot{e}_i + k_{2i}e_i \tag{17}$$

substituting (17) in (16) will give:

$$g_{2i} = \frac{1}{k_{1i}}(\dot{g}_{1i} + c_{1i}g_{1i}) \tag{18}$$

assuming the 1st Lyapunov positive definite V_{2i} with time derivative negative semidefinite as in (19):

$$V_{2i} = \tfrac{1}{2}(g_{1i}^2 + g_{2i}^2) \tag{19}$$

differentiating (18) will give:

$$\dot{V}_{2i} = g_{1i}\dot{g}_{1i} + g_{2i}\dot{g}_{2i} \tag{20}$$

substituting $\dot{g}_{1i}$ and $\dot{g}_{2i}$ in (20):

$$\dot{V}_{2i} = g_{2i}\left[\begin{array}{l}\left(k_{1i}^2 + \frac{c_{1i}k_{2i}}{k_{1i}}\right)e_i + \left(c_{1i} + \frac{k_{2i}}{k_{1i}}\right)\dot{e}_i \\ +k_{1i}k_{2i}\int e_i dt - g_i + \frac{U_{1i}}{m_i}\cos\theta_i\cos\phi_i - \ddot{z}_{di}\end{array}\right] \\ -g_{1i}\left[c_{1i}k_{1i}e_i + c_{1i}k_{2i}\int e_i dt\right] \tag{21}$$

$$\dot{V}_{2i} = -\frac{c_{2i}}{k_{1i}}[\dot{g}_{1i} + c_{1i}g_{1i}] \\ = -(c_{2i})\dot{e}_i - (A_i)e_i - (B_i)\int e_i dt \tag{22}$$

where

$$A_i = \left(c_{1i}c_{2i} + \frac{c_{2i}k_{2i}}{k_{1i}}\right),\ B_i = \left(\frac{c_{1i}c_{2i}k_{2i}}{k_{1i}}\right) \tag{23}$$

where c_{2i}, A_i, and B_i are positive parameters.

Equation (20) is negative when the required control is formulated as:

$$U_{1i} = \frac{m_i}{\cos\theta_i\cos\phi_i}\left[\begin{array}{l}-\left(k_{1i}^2 + \frac{c_{1i}k_{2i}}{k_{1i}} + c_{1i}c_{2i} + \frac{c_{2i}k_{2i}}{k_{1i}}\right)e_i \\ -\left(c_{1i} + \frac{k_{2i}}{k_{1i}} + c_{2i}\right)\dot{e}_i \\ -\left(k_{1i}k_{2i} + \frac{c_{1i}c_{2i}k_{2i}}{k_{1i}}\right)\int e_i dt + g_i + \ddot{z}_{di}\end{array}\right] \tag{24}$$

in accordance with backstepping approach, the altitude control and the position control (U_{1i}, u_{xi}, u_{yi}) is assumed as:

$$U_{1i} = \frac{m_i}{\cos x_{1i}\cos x_{3i}}(g_i + g_{7i} - \alpha_{7i}(g_{8i} + \alpha_{7i}g_{7i}) - \alpha_{8i}g_{8i}) \\ u_{xi} = \frac{m_i}{U_{1i}}(g_{9i} - \alpha_{9i}(g_{10i} + \alpha_{9i}g_{9i}) - \alpha_{10i}g_{10i}) \\ u_{yi} = \frac{m_i}{U_{1i}}(g_{11i} - \alpha_{11i}(g_{12i} + \alpha_{11i}g_{11i}) - \alpha_{12i}g_{12i}) \tag{25}$$

3.2. Adaptive neuro-fuzzy inference system approach

FL and synthetic ANN are normal complementary stuff in constructing hybrid intelligent systems (Werbos, 1992). ANN can be considered as a low-level computational framework which acts well when interacting with raw data (Muslimi et al., 2006). On the other hand, FL treats with logic on a higher-level, utilizing linguistic data obtained from range experts (Gupta).

However, fuzzy systems cannot adapt themselves in new surroundings and haven't the learning capability which characterized the ANN approach (Yong & Tuan, 2006). The incorporation of FL and ANN enable combining the decision making capabilities of FL with learning capabilities of ANN (Kumari & Sunita, 2013). Consequently, the results of the FL and ANN incorporation sum up their superiorities and scale back the constraints of each system. The incorporation of FL and ANN was introduced primarily by Jang (1993).

Generally, the neuro-fuzzy intelligent systems can be utilized cooperatively, concurrently, or as a hybrid system. In the cooperative technique, the learning capabilities of the ANN are used to construct the base foundation in the fuzzy membership functions from the training data, then the fuzzy part works separately. In the concurrent technique, the FL and ANN work in such a parallel way and facilitate one another to identify the required parameters. In the hybrid technique, the architectures of both FL and ANN are almost the same which facilitates applying the learning algorithms of the ANN to the FL (Ferdaus et al., 2018).

The ANFIS structure is constructed on two main pillar parameter sets: premise and consequent parameters. Training approach of ANFIS controller can be achieved by determining those couple set of parameters using optimization technique (Karaboga & Kaya, 2019). ANFIS utilizes the input-output existing data pairs throughout training phase. The fuzzy IF-THEN rules foundation are obtained and linked to each other constructing the hybrid neuro-fuzzy approach (Al-Fetyani et al., 2021).

A simple paradigm of the neuro-fuzzy framework of couple of inputs, and one output based on Takagi-Sugeno model is demonstrated in Figure 3.

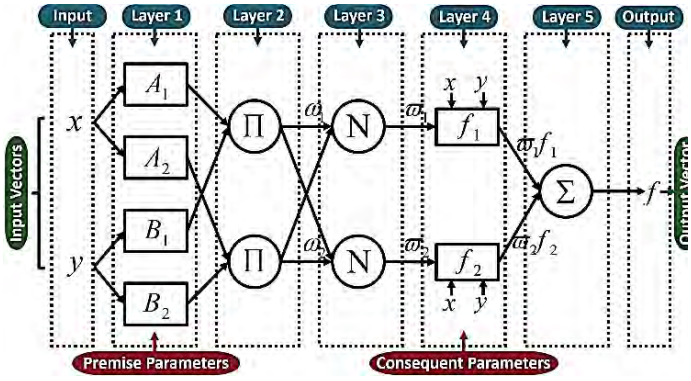

Figure 3. ANFIS paradigm architecture.

Familiar rule sets of couple of fuzzy IF-THEN rules in the ANFIS architecture.

First rule: if x and y represent A_1 and B_1 respectively, so

$$f_1 = p_1 x_i + q_1 y_i + r_1 \tag{26}$$

second rule: if x and y represent A_2 and B_2 respectively, so

$$f_2 = p_2 x_i + q_2 y_i + r_2 \tag{27}$$

assuming, for layer m and n_{th} nodes the output is $O_{m,n}$.

Layer 1: is the fuzzification layer.

Every node is an adaptive one during this layer. The outcome function for n_{th} node is:

$$O_{1,n} = \mu A_n(x_i) \text{ for } n = 1,2. \tag{28}$$

$$O_{1,n} = \mu B_n(y_i) \text{ for } n = 3,4. \tag{29}$$

The parameters that completely identify the membership degree functions $\mu A_n(x)$ and $\mu B_n(y)$ to be bell shaped are called antecedent parameters, like

$$\mu A_n(x_i) = \frac{1}{\left(1 + \left|\frac{x_i - c_n}{a_n}\right|^{2b_n}\right)} \tag{30}$$

where $\{a_n, b_n, c_n\}$ is a set of parameters.

Those parameters are called premise parameters as well in this layer.

Layer 2: is the ruler layer.

Every node is a steady one stamped Π during this layer. It works as a multiplier for the incoming signals, like

$$O_{2,n} = \omega_n = \mu A_n(x_i) * \mu B_n(y_i) \tag{31}$$

where ω_n is the second layer's output.

Output of every node outlines believability of this rule.

Layer 3: is the normalization layer.

Every node is a steady one stamped N during this layer. The firing strength ratio of the rules is calculated by the n_{th} nodes, like

$$O_{3,n} = \varpi_n = \frac{\omega_n}{\omega_1 + \omega_2} \text{ for } n = 1,2. \tag{32}$$

where ϖ_n is the third layer's output.

The outcomes of this layer are classified as normalized firing forces.

Layer 4: is the defuzzification layer.

Every node is an adaptive one during this layer. The outcome of this layer for n_{th} node is:

$$O_{4,n} = \varpi_n f_n = \varpi_n (p_n x_i + q_n y_i + r_n) \tag{33}$$

where $\{p_n, q_n, r_n\}$ is a set of parameters.

Those parameters are called Consequent parameters as well in this layer.

Layer 5: is the summation layer.

The one and only node is a steady one during this layer. It calculates the summation of the aggregate incoming signals.

$$O_{5,n} = \sum_n \varpi_n f_n = \frac{\sum_n \omega_n f_n}{\sum_n \omega_n} = \varpi_1 f_1 + \varpi_2 f_2 \tag{34}$$

In the presence of the premise parameters as a given, ANFIS results can be re-written as a linear aggregation of consequent parameters, like

$$O_{5,n} = \sum_n \varpi_n f_n = \frac{\sum_n \omega_n f_n}{\sum_n \omega_n} = \frac{\omega_1 f_1}{\omega_1 + \omega_2} + \frac{\omega_2 f_2}{\omega_1 + \omega_2}$$

$$= \frac{\omega_1}{\omega_1 + \omega_2} f_1 + \frac{\omega_2}{\omega_1 + \omega_2} f_2 = \varpi_1 f_1 + \varpi_2 f_2 \tag{35}$$

from (26) and (27):

$$\sum_n f_n = \left(\sum_n p_n x + q_n y + r_n\right) = f_1 + f_2 \\ = \left(p_1 x + q_1 y + r_1\right) + \left(p_2 x + q_2 y + r_2\right) \quad (36)$$

substituting (36) in (35):

$$O_{5,n} = \varpi_1\left(p_1 x + q_1 y + r_1\right) + \varpi_2\left(p_2 x + q_2 y + r_2\right) \\ = \left(\varpi_1 x\right) p_1 + \left(\varpi_1 y\right) q_1 + \left(\varpi_1 r_1\right) \\ + \left(\varpi_2 x\right) p_2 + \left(\varpi_2 y\right) q_2 + \left(\varpi_2 r_2\right) = R.\theta \quad (37)$$

where $\{p_1, q_1, r_1, p_2, q_2, r_2\}$ is a set of consequent parameters.

Assume $\theta = \{p_1, q_1, r_1, p_2, q_2, r_2\}$ (38)

getting an R from (5). So, optimal evaluation $\widehat{\theta}$ can be obtained by Least Square (LS) technique by estimating the minimum meaning of $\|R.\theta - f\|^2$. As a result:

$$\hat{\theta} = \left(A^T A\right)^{-1} A^T f \quad (39)$$

evaluated output $\widehat{f}$ can be obtained by:

$$\widehat{f} = A.\hat{\theta} \quad (40)$$

so, premise and consequent parameters can be computed by meaning value of the root-mean square error (RMSE) by:

$$RMSE = \sqrt{\sum_{k=1}^{t}\left(\widehat{f_k} - f_k\right)^2 / t} \quad (41)$$

intermixture of back propagation (BP) criteria and LS technique can regulate premise and consequent parameters of the ANFIS.

This intermixture is used as a hybrid learning technique. In the intermixture principle, there are forward-way and invert-way (Navarro & Akhi-Elarab, 2013).

In forward-way, the output of the fourth layer is calculated; LS technique is then utilized to determine consequent parameters.

In the invert-way section, error signals manipulate invert transmission, and premise parameters are updated using PB criteria.

Throughout forward-way, the output value $O_{5,n}$ can be obtained for set of adopted incoming values of training data by resolving the consequent parameters $\{p_n, q_n, r_n\}$ during the learning process.

Due to principles of LS technique, the expected error values of the training data are computed through the output value $O_{5,i}$ calculation process.

Due to most gradient techniques, this error will be inversely restored and precise the premise parameters.

Throughout the precision process of these parameters, adjustment of membership function diagrams is unceasingly recognized, anticipating achieving the aim of getting least output error throughout iteration process.

Every learning procedure to ANFIS structure contains premise parameter learning stage and consequent parameter learning stage (Liu & Zhou, 2017).

Flow chart of intelligence formation algorithm is clarified in Figure 4.

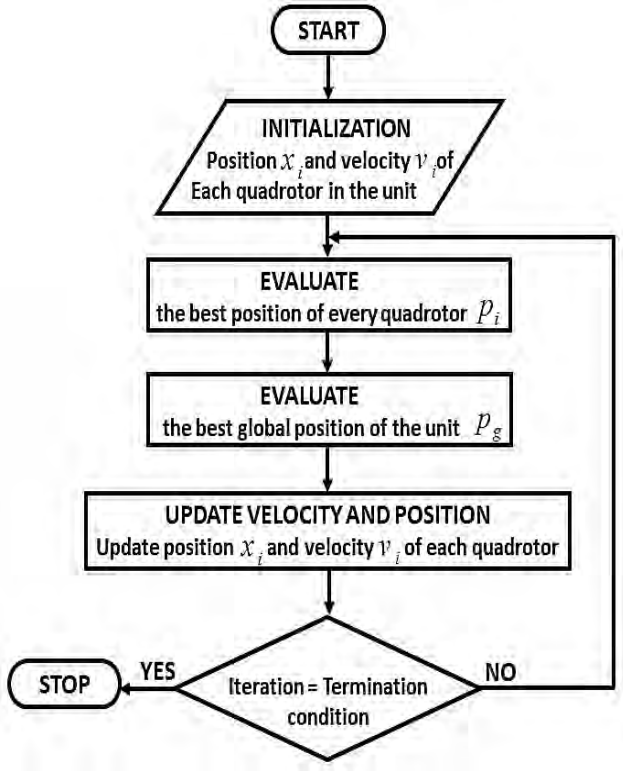

Figure 4. Flow chart of formation algorithm.

4. Simulation results

A simulation atmosphere is settled under "SIMULINK-MATLAB" to approve the offered control strategy. The simulation is built on the entire non-linear model of a group of three quadrotors introduced by Equation (7). Each quadrotor in the underlying system contains two stages of controllers. The backstepping controller represents the higher controller where it controls the altitude and the position. The ANFIS controller represents the lower controller where it receives the altitude and the position from the backstepping to acquire the attitude controller to turn over the angels to execute the desired altitude and position. Also, it transmits the proper control signal for the propellers to accomplish the whole designed mission respecting the desired separating distance and desired velocity.

The designed ANFIS controller is composed of 16 membership functions and 16 fuzzy rules as shown in Figure 5.

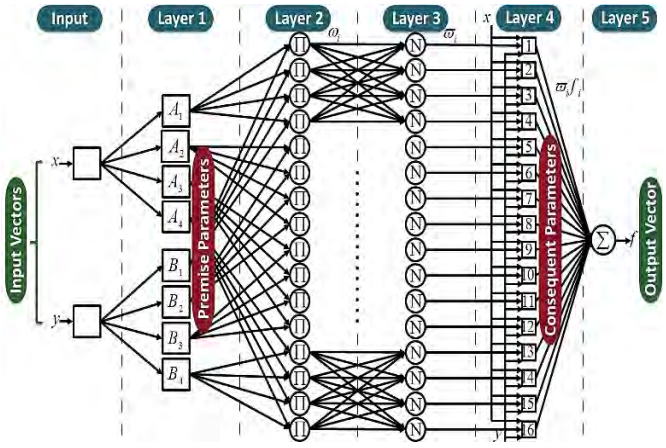

Figure 5. ANFIS topology.

The ANFIS paradigm is created using MATLAB's ANFIS GUI editor. The grid partition method generates optimized rules. The ANFIS paradigm architecture has the subsequent information as shown in Table 1.

Table 1. Subsequent information of ANFIS model architecture.

Type	Number
Nodes	53
Power (kW)	48
linear parameters	24
Total parameters	72
Training data pairs	525
Checking data pairs	525
Fuzzy rules	16

The neural network uses the hybrid technique to minimize the error by optimizing the parameters and the membership functions.

This hybrid backstepping-ANFIS controller is studied earlier with a backstepping- backstepping controller for the selfsame framework in (Mahfouz et al., 2018). For training approach, the input/output data sets of various points of operation are exercised.

The obtained data sets are divided equally; half of them is used for training, while the others are used for checking. Hybrid optimization technique generates the FIS structure based on obtained data sets. For the training approach, ANFIS finishes training at epoch two with zero tolerance.

For roll control channel, the error input is ranged from -0.3123 to +0.0156, the error derivative is ranged from -0.889 to +0.05057, and the output for roll moment is ranged from -6.844 to +0.9527. For pitch control channel, the error input ranges from -0.003404 to +0.4045, the error derivative is ranged from -0.6946 to +0.15, and the output for pitch moment is ranged from -24.11 to +3.344. Finally, for yaw control channel, the error input is ranged from -0.3 to +0.04915, the error derivative is ranged from -3.306 to +1.044, and the output for yaw moment is ranged from -67.58 to +199.6.

The ANFIS topology consists of four hidden layers having two inputs, one output, four premise parameters for each input, and sixteen membership functions that create sixteen rules in each ANFIS topology. Path trajectory is designed to test the ability of the underlying hybrid controller to pursue the path trajectory reserving the desired formation configuration of the group members of the cooperative quadrotors. The group is composed of three quadrotors. Every quadrotor began from various points of operation.

- Assumption 1

All the cooperative quadrotors under-study are rigids and have the same mathematical model.

- *Assumption 2*

The group of cooperative quadrotors under-study consists of three quadrotors in a triangular formation. Each follower quadrotor keeps a separating distance 5 m in the X and Y axis with respect to the leader, and a distance 10 m in the Y axis between each other.

- *Assumption 3*

All the altitude of the three cooperative quadrotors is constant.

The validation of the proposed controller is presented through the simulation results recorded in couple of scenarios in the presence and absence of stationary and moving obstacles.

- Scenario 1

In this scenario, a group of three cooperative quadrotors tracks a reference path along the X-axis in a triangular shape

in a free obstacle environment. The initial position of the quadrotors are as follows: leader = (0,0), Follower 1 = (7,5) and Follower 2 = (-7,-7). The path of the group in the X-direction is demonstrated in Figure 6, where the followers' quadrotors respect the separating distance with respect to the leader in order to pursue a pre-planned trajectory. Moreover, Figure 7 demonstrates the velocity component in the X-axis for each member of the group respecting the constrain velocity $|V_x| \leq 2 \quad (m/s)$ and the pitch control for all the team members is demonstrated in Figure 8.

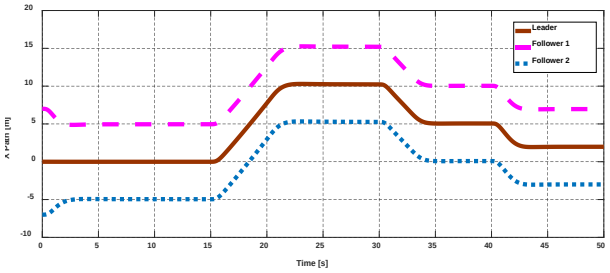

Figure 6. Trajectory of a group of cooperative quadrotors. Along X-axis.

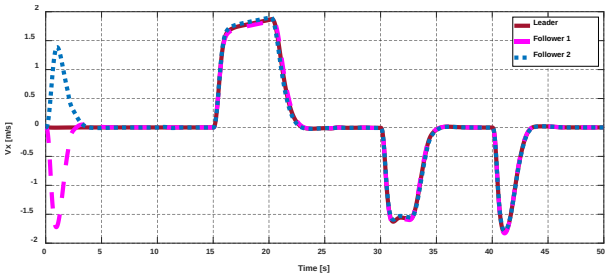

Figure 7. The velocity components for the cooperative quadrotors in X-axis.

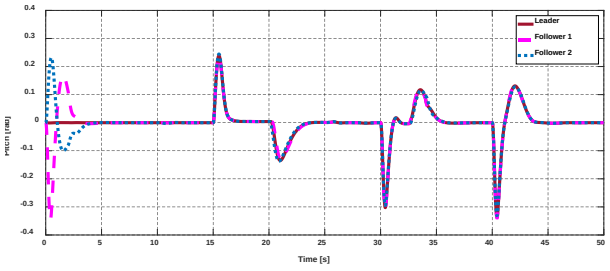

Figure 8. Pitch control for the three cooperative quadrotors.

The trajectory of the three cooperative quadrotors along the Y- axis is shown in Figure 9. The two followers succeeded in achieving the desired separating distance (10 m) between each other and the desired separating distance (5 m) with respect to the leader quadrotor. Moreover, Figure 10 demonstrates the velocity component in the Y-axis of each member of the group respecting the constrain $|V_y| \leq 2 \quad (m/s)$ and the roll control for all the group members is demonstrated in Figure 11.

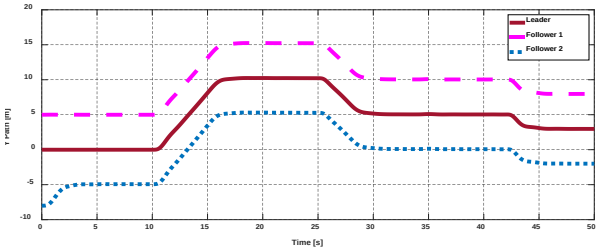

Figure 9. Trajectory of a group of cooperative quadrotors along Y-axis.

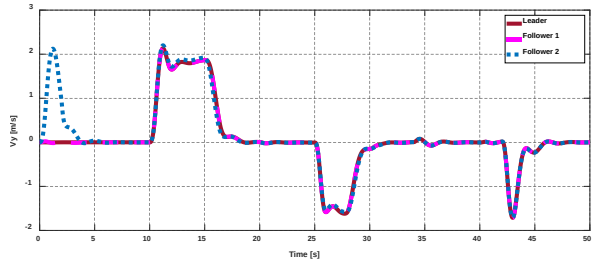

Figure 10. Velocity components for the cooperative quadrotors in Y-axis.

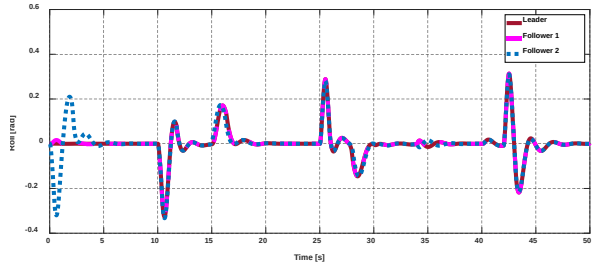

Figure 11. Roll control for the cooperative quadrotors.

The position of the quadrotors along the Z- axis is represented in Figure 12. Figure 13 represents the velocity components of the three quadrotors along the Z-axis. Finally, the yaw control for the three cooperative quadrotors is demonstrated in Figure 14.

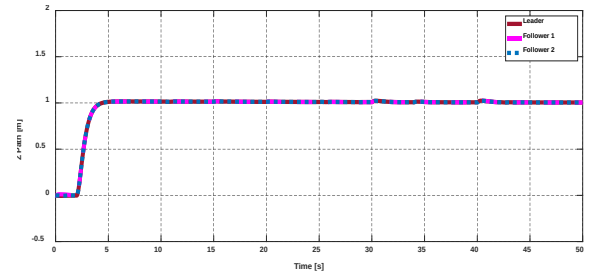

Figure 12. Trajectory followed by a group of cooperative quadrotors along Z-axis.

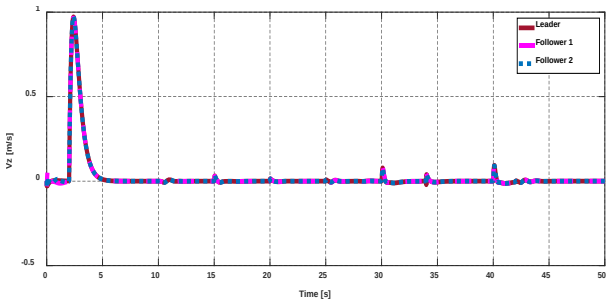

Figure 13. Velocity components in Z - axis.

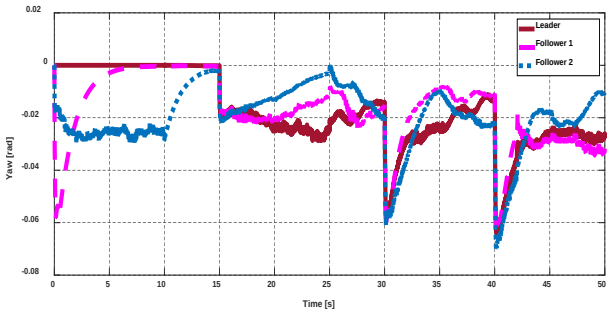

Figure 14. Yaw controls the three cooperative quadrotors.

- *Scenario 2*

In this scenario, the proposed controller is evaluated to solve the formation problem for a group of cooperative quadrotors in static/dynamic obstacles-loaded environment.

A couple of obstacles avoidance techniques are applied to guarantee the safety of all members of the group during tracking a reference desired trajectory in presence of stationary and moving obstacles in an obstacle-loaded dynamic environment.

Stationary obstacle avoidance approach was developed in (Mahfouz et al., 2018; Mahfouz et al., 2019), while moving obstacle avoidance approach was introduced in (Mahfouz, Hafez, Ashry & Elnashar, 2020; Mahfouz, Hafez, Azzam, et al., 2020).

Stationary obstacles

In order to demonstrate the underlying controller's ability to pursue the required route in an obstacle-filled environment, obstacles are designed as a rectangle shape. It is assumed that the quadrotors altitudes constant for simplification. Then it would reduce the difficulty of tracking the trajectory to a 2D problem. Two security zones are designed for complete flight safety reasons, by a 20m-radius safety zone and a 10m-detaching range identifying protected zone among every follower and the leader UAV (Mahjri et al., 2015). These safety zones are activated when an obstacle is captured on the border of the safety zones. This causes an interruption for tracking the trajectory making a half circle maneuver to bypass the captured obstacle, and then resuming tracking the original trajectory. As sh the obstacle avoidance algorithm represented in this work guarantees the safety of all members of the fleet. In Figure 15, the leader of a team of cooperative quadrotors senses the presence of a stationary obstacle. The team reconfigures from a triangular formation into a line formation with a separation safety distance of 10 m between every successive quadrotor.

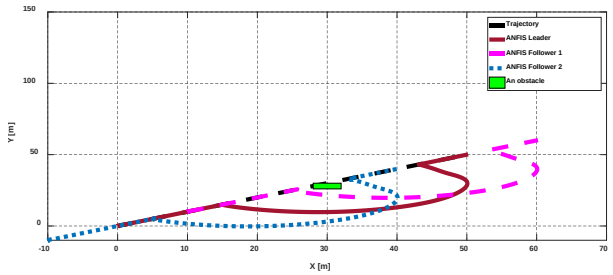

Figure 15. The trajectory of the group of cooperative quadrotors in the presence of a stationary obstacle in XY-axis.

The designed obstacle avoidance technique in motion planning offered in this paper is a simple mathematical solution; this technique calculated the dimensions and the vertices of the captured obstacles to prevent collision.

Assume $X_{Ob\min}$ and $X_{Ob\max}$ symbolizes the minimum and maximum dimensions of the obstacle edges in x -axis. Similarly, $\Upsilon_{Ob\min}$ and $\Upsilon_{O\max}$ symbolizes the minimum and maximum dimensions of the obstacle edges in y -axis as shown in Figure 16.

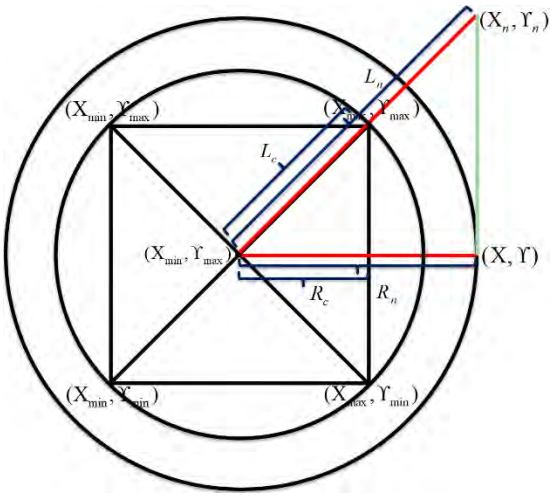

Figure 16. A mathematical solution for obstacle avoidance.

Assume (x_c, y_c) the midpoint of the captured obstacle, this point can be acquired by equations (42, 43):

$$X_c = (X_{Ob\min} + X_{Ob\max})/2 \quad (42)$$

$$\Upsilon_c = (\Upsilon_{Ob\min} + \Upsilon_{Ob\max})/2 \quad (43)$$

the radius R_c of the circumscribed circle can be calculated by equation (44):

$$R_c = 0.5*\sqrt{(X_{Ob\max} - X_{Ob\min})^2 + (\Upsilon_{Ob\max} - \Upsilon_{Ob\min})^2} \quad (44)$$

the new trajectory can be generated by solving the drawn path mathematically through the mapping produced path from the series of (X, Υ) points to a new series of (X_n, Υ_n) points after gathering a safety distance δ_d as in Equations (45) and (46).

$$X_n = X_c + (X - X_c)*R_c / \delta_d \quad (45)$$

$$\Upsilon_n = \Upsilon_c + (\Upsilon - \Upsilon_c)*R_c / \delta_d \quad (46)$$

The new generated trajectory enables the group of the UAVs to avoid collision with the captured obstacle. The designed controller succeeded in controlling each unmanned quadrotor in the troop in a decentralized manner guaranteeing the reserving of the desired geometric formation in XYZ-plane is shown in Figure 17.

Figure 18 represents the separation distance between the leader and the Follower 1 and the separation distance between Follower 1 and Follower 2.

The proposed control approach was compared with a backstepping-backstepping controller. Figure 19 and Figure 20 demonstrate the trajectories of cooperative quadrotors in the presence of a single stationary obstacle in XY-axis and XYZ-plane, respectively. The two control approaches succeeded in guaranteeing the safety of all the members of the group.

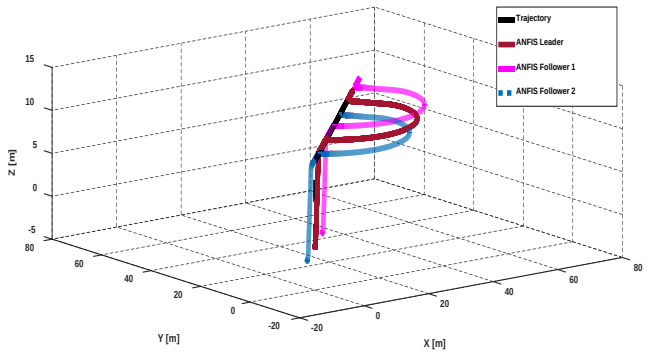

Figure 17. The trajectory of the group of cooperative quadrotors in the presence of a stationary obstacle in XYZ-plane.

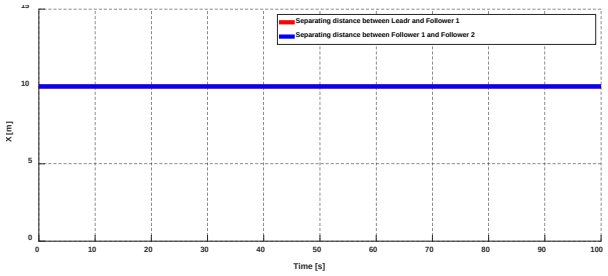

Figure 18. the separation distance between the leader and the Follower 1 and the separation distance between Follower 1 and Follower 2 in X-axis.

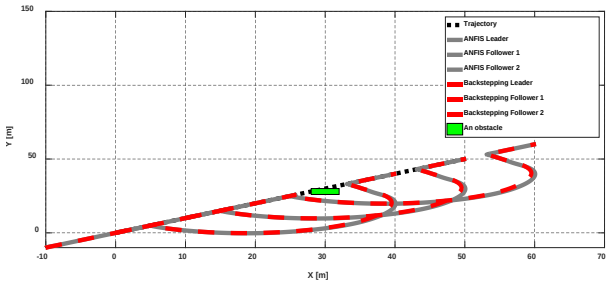

Figure 19. Trajectories of cooperative quadrotors in the presence of a stationary obstacle in XY-axis.

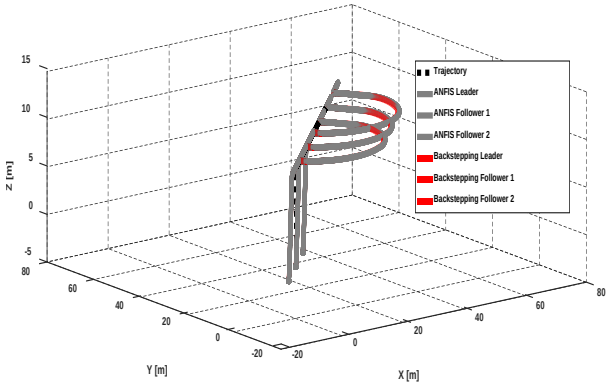

Figure 20. Trajectories of cooperative quadrotors in the presence of a stationary obstacle in XYZ-plane.

Dynamic obstacles

In this subsection, the proposed hybrid control approach will be applied on three cooperative quadrotors in the presence of dynamic obstacles as shown in Figure 21.

The first obstacle is moving along the desired trajectory with a lower speed while the second obstacle is moving in an opposite direction to collide with the group.

The proposed control approach was compared with a backstepping – backstepping approach. Figure 22 and Figure 23 demonstrate the trajectories of cooperative quadrotors in the presence of a couple dynamic obstacles in XY-axis and XZ-axis, respectively.

The path of the group cooperative quadrotors in the presence of couple dynamic obstacles in XYZ- plane is introduced in Figure 24.

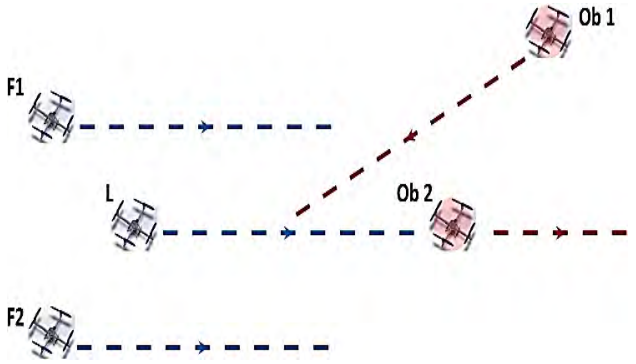

Figure 21. A couple of UAVs acting as moving obstacles intersecting the trajectory of the cooperative quadrotors.

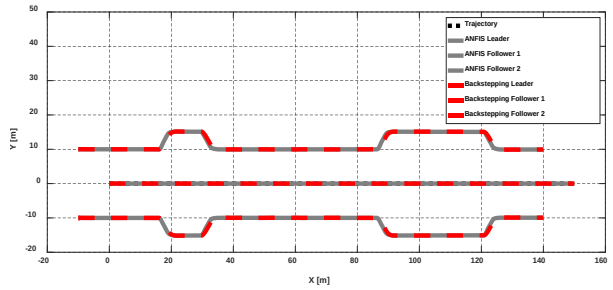

Figure 22. Trajectories of cooperative quadrotors in the presence of couple of moving obstacles in XY-axis.

Figure 23 demonstrates the ANFIS controller versus backstepping controller in the presence of a couple of moving obstacles in XYZ-plane.

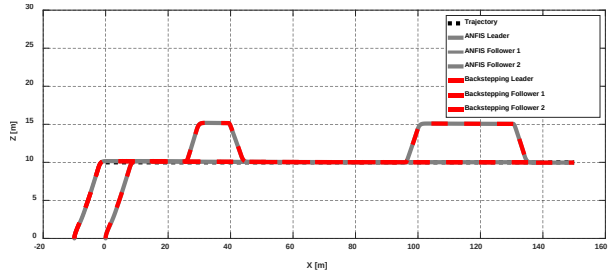

Figure 23. Trajectories of cooperative quadrotors in the presence of couple of moving obstacles in XZ-axis.

Finally, all the simulation results presented in Scenario 1 and Scenario 2 show that the proposed hybrid controller achieves a good track to pre-planned trajectories in the presence and absence of both stationary and moving obstacles.

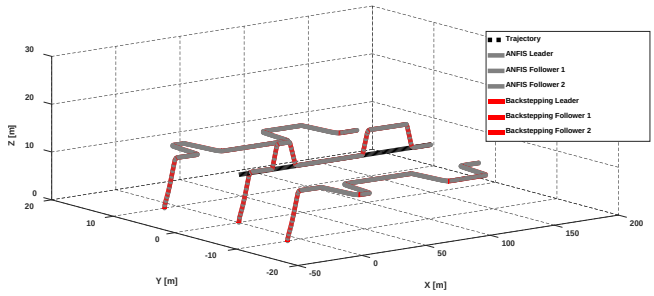

Figure 24. The path of three cooperative quadrotors in the presence of couple of moving obstacles in XYZ-plane.

5. Stability analysis of hybrid controller

For ease of control, the accurate perfect quadrotor model is reduced by decreasing the outer forces and torques to take on the real-time restrictions of the incorporated control cycle (Wierema, 2008).

In this manner, the 12-states and 6-DOF framework i of the quadrotor can be reworded in state-space definition $\dot{X}_i = f(X_i, \eta_i)$ taking into account the inputs parameters η_i and the state parameters X_i of the framework as (Bouabdallah & Siegwart, 2007):

$$X_i = [\phi_i, \dot{\phi}_i, \theta_i, \dot{\theta}_i, \psi_i, \dot{\psi}_i, z_i, \dot{z}_i, x_i, \dot{x}_i, y_i, \dot{y}_i]^T \quad (47)$$

assuming the following:

$$\begin{aligned} x_{1i} &= \phi_i & x_{7i} &= z_i \\ x_{2i} &= \dot{x}_{1i} = \dot{\phi}_i & x_{8i} &= \dot{x}_{7i} = \dot{z}_i \\ x_{3i} &= \theta_i & x_{9i} &= x_i \\ x_{4i} &= \dot{x}_{3i} = \dot{\theta}_i & x_{10i} &= \dot{x}_{9i} = \dot{x}_i \\ x_{5i} &= \psi_i & x_{11i} &= y_i \\ x_{6i} &= \dot{x}_{5i} = \dot{\psi}_i & x_{12i} &= \dot{x}_{11i} = \dot{y}_i \end{aligned} \quad (48)$$

$$\eta_i = \begin{bmatrix} \eta_{1i} & \eta_{2i} & \eta_{3i} & \eta_{4i} \end{bmatrix}^T \quad (49)$$

by combining Equation (4) with Equations (47) and (49). The reduced quadrotor model is presented in (50):

$$f\ (X_{\ i}, \eta_i) = \begin{pmatrix} \dot{\phi}_i \\ \dot{\theta}_i \dot{\psi}_i a_{1i} + \dot{\theta}_i a_{2i} \Omega_{ri} + b_{1i} \eta_{2i} \\ \dot{\theta}_i \\ \dot{\phi}_i \dot{\psi}_i a_{3i} - \dot{\phi}_i a_{4i} \Omega_{ri} + b_{2i} \eta_{3i} \\ \dot{\psi}_i \\ \dot{\phi}_i \dot{\theta}_i a_{5i} + b_{3i} \eta_{4i} \\ \dot{z}_i \\ g - \frac{1}{m_i} (\cos\phi_i \cos\theta_i) \eta_{1i} \\ \dot{x}_i \\ u_{xi} \frac{1}{m_i} \eta_{1i} \\ \dot{y}_i \\ u_{yi} \frac{1}{m_i} \eta_{1i} \end{pmatrix} \quad (50)$$

were

$$\begin{cases} a_{1i} = (I_{yi} - I_{zi}) / I_{xi} & a_{2i} = -J_{ri} / I_{xi} \\ a_{3i} = (I_{zi} - I_{xi}) / I_{yi} & a_{4i} = J_{ri} / I_{yi} \\ a_{5i} = (I_{xi} - I_{yi}) / I_{zi} & b_{1i} = l_i / I_{xi} \\ b_{2i} = l_i / I_{yi} & b_{3i} = 1 / I_{zi} \end{cases} \quad (51)$$

from (50), the quadrotor rotation rate can be defined as:

$$\begin{pmatrix} \dot{x}_{2i} \\ \dot{x}_{4i} \\ \dot{x}_{6i} \end{pmatrix} = \begin{pmatrix} a_{1i} x_{4i} x_{6i} + a_{2i} x_{4i} \Omega_{ri} + b_{1i} \eta_{2i} \\ a_{3i} x_{2i} x_{6i} + a_{4i} x_{2i} \Omega_{ri} + b_{2i} \eta_{3i} \\ a_{5i} x_{2i} x_{4i} + b_{3i} \eta_{4i} \end{pmatrix} \quad (52)$$

Equations (4) and (52) empower configuring the quadrotor attitude control. Neglecting the gyroscopic parameters in (52):

$$\begin{pmatrix} \dot{x}_{2i} \\ \dot{x}_{4i} \\ \dot{x}_{6i} \end{pmatrix} = \begin{pmatrix} a_{1i} x_{4i} x_{6i} + b_{1i} \eta_{2i} \\ a_{3i} x_{2i} x_{6i} + b_{2i} \eta_{3i} \\ a_{5i} x_{2i} x_{4i} + b_{3i} \eta_{4i} \end{pmatrix} \quad (53)$$

supposing $\eta^*_{2i}, \eta^*_{3i} and \quad \eta^*_{4i}$ to obtain a linear framework where:

$$\begin{cases} \eta_{2i} = f_{2i}(x_{2i}, \quad x_{4i}, \quad x_{6i}) + \eta^*_{2i} \\ \eta_{3i} = f_{3i}(x_{2i}, \quad x_{4i}, \quad x_{6i}) + \eta^*_{3i} \\ \eta_{4i} = f_{4i}(x_{2i}, \quad x_{4i}, \quad x_{6i}) + \eta^*_{4i} \end{cases} \quad (54)$$

the nonlinear feedback for linearization can be acquired by:

$$\begin{cases} f_{2i}(x_{2i}, x_{4i}, x_{6i}) = \frac{1}{b_{1i}} (\beta_{2i} x_{2i} - a_{1i} x_{4i} x_{6i}) \\ f_{3i}(x_{2i}, x_{4i}, x_{6i}) = \frac{1}{b_{2i}} (\beta_{3i} x_{4i} - a_{3i} x_{2i} x_{6i}) \\ f_{4i}(x_{2i}, x_{4i}, x_{6i}) = \frac{1}{b_{3i}} (\beta_{4i} x_{6i} - a_{5i} x_{2i} x_{4i}) \end{cases} \quad (55)$$

utilizing (49) leads to transform (47) into linear and decoupled framework as:

$$\begin{pmatrix} \dot{x}_{2i} \\ \dot{x}_{4i} \\ \dot{x}_{6i} \end{pmatrix} = \begin{pmatrix} \beta_{2i} x_{2i} + \frac{1}{b_{1i}} \eta^*_{2i} \\ \beta_{3i} x_{4i} + \frac{1}{b_{2i}} \eta^*_{3i} \\ \beta_{4i} x_{6i} + \frac{1}{b_{3i}} \eta^*_{4i} \end{pmatrix} \quad (56)$$

considering $U^*_{2i} = U^*_{3i} = U^*_{4i} = 0$ and the assumed points of operation $x_{2i} = x_{4i} = x_{6i} = 0$; the generated linearized closed-loop framework is constant with or without the gyroscopic parameters in (51).

Various methods discuss the stability of complex systems such as Routh–Hurwitz method, Bode diagram, Nyquist diagram, root-locus method, the Nichols chart, and Lyapunov stability criterions (Shinners, 1998). The Lyapunov stability offers precise solutions close to the point of equilibrium of non-linear system. Exponential stability in Lyapunov guarantees a low decay rate which show an estimation of how rapidly the solutions converge (Fichera, 2013; Totoki et al., 2009). Because of that Lyapunov stability criterions have been chosen to analyze and confirm the stability of the offered hybrid controller.

To prove the stability, the Lyapunov function $V_i(x_{2i}, x_{4i}, x_{6i})$ for the attitude controller G_{ci} and positive designated about the point of operation (Wu, 2009):

$$V_i(x_{2i}, x_{4i}, x_{6i}) = 0.25(x^4_{2i} + x^4_{4i} + x^4_{6i}) \quad (57)$$

the initial derivative of the Lyapunov function $\dot{V}_i$ is resolved by exercising (52), (54), and (55). In addition, if $a_{1i} = -a_{3i}$ and $a_{5i} = 0$, a standard quadrotor cross configuration with $I_{xi} = I_{yi}$ is gained. So, $\dot{V}_i$ can be reached by:

$$\begin{aligned} \dot{V}_i &= x_{2i} \dot{x}_{2i} + x_{4i} \dot{x}_{4i} + x_{6i} \dot{x}_{6i} \\ &= K_{2i} x^2_{2i} + K_{3i} x^2_{4i} + K_{4i} x^2_{6i} \end{aligned} \quad (58)$$

it is obvious that $\dot{V}_i$ is free from gyroscopic parameters as well. $\dot{V}_i$ is negative if $K_{2i}, K_{3i}, K_{4i} < 0$. The points of operation concerning the linearized order of feedback are therefore asymptotically stable.

To check the stability of the proposed hybrid controller, an equal uniformed pulse disturbance is applied in different intervals of times to each quadrotor in the group as demonstrated in Figure 25.

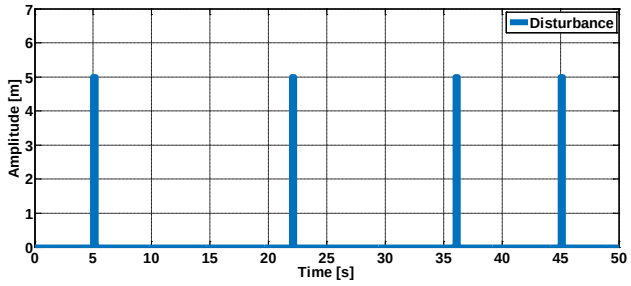

Figure 25. Impulse disturbance.

Like Scenario 1 in Section IV, a group of three cooperative quadrotors moves along the X-axis with a desired separation distance in a free obstacle environment forming a triangular formation.

The sudden disturbances shown in Figure 25 are applied to the members of the group. Figure 26 demonstrates the path trajectory for the group of the cooperative quadrotors following a desired path along the X-axis. The result shows the ability of the hybrid controller to reject the applied disturbance.

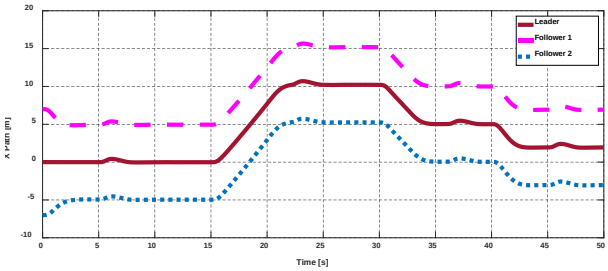

Figure 26. Trajectory of a group of cooperative quadrotors along X-axis under the effect of sudden disturbances.

The velocity components along the X-axis of the three quadrotors and their pitch control are demonstrated in Figure 27 and Figure 28 respectively. The results show that the hybrid controller succeeded in rejecting the effect of the sudden disturbances and guarantees the desired velocity.

Similarly, Figure 29, Figure 30, and Figure 31 demonstrate the trajectories of the three cooperative quadrotors along Y-axis, their velocity components and their roll control, respectively.

The results validate the success of the introduced hybrid control approach to reject the effect of the impulse and guarantee the desired separating distance and velocity.

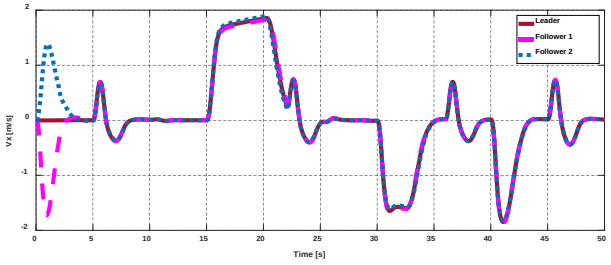

Figure 27. Velocity components along X –axis under the effect of sudden disturbances.

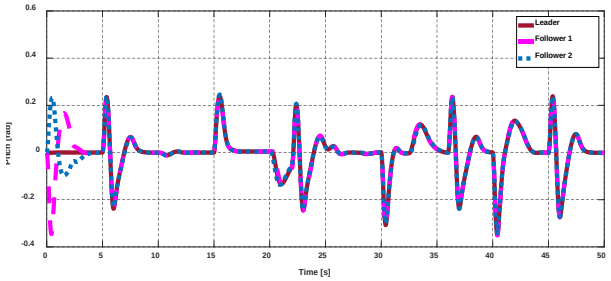

Figure 28. Pitch control for the cooperative quadrotors under the effect of sudden disturbances.

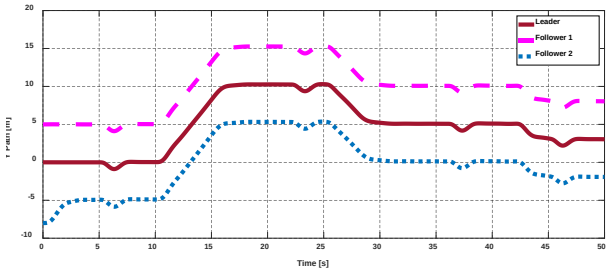

Figure 29. Trajectory of a group of cooperative quadrotors along Y-axis under the effect of sudden disturbances.

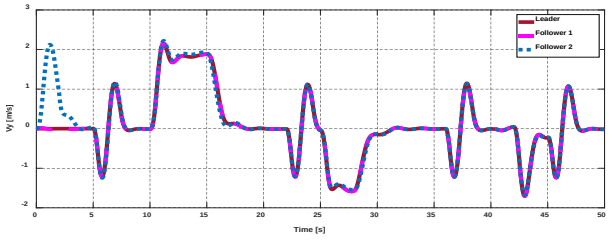

Figure 30. Velocity components along Y –axis under the effect of sudden disturbances.

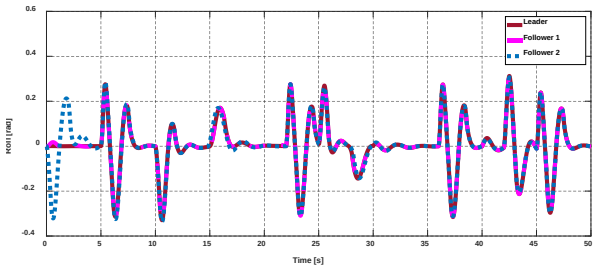

Figure 31. Roll control for the cooperative quadrotors under the effect of sudden disturbances.

However, the altitude of the three cooperative quadrotors is constant, sudden disturbance was applied to investigate their effects on the quadrotors. Figure 32, Figure 33, and Figure 34 demonstrate the trajectories of the three cooperative quadrotors along Z-axis, their velocity components and their yaw control, respectively. The results show the capacity of the hybrid controller to dismiss the applied disturbance.

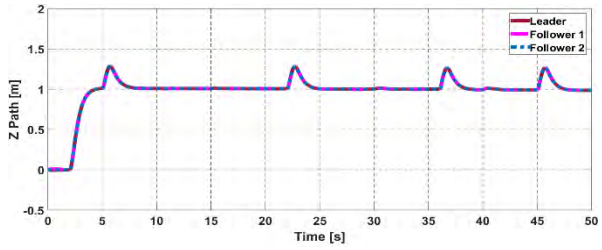

Figure 32. Trajectory of a group of cooperative quadrotors along Z-axis under the effect of sudden disturbances.

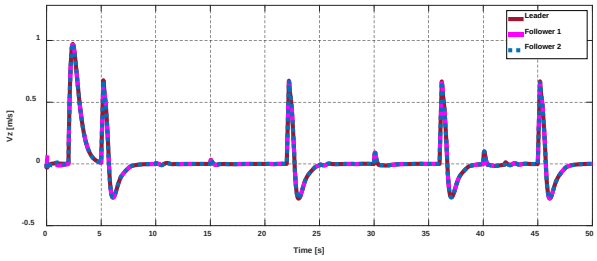

Figure 33. Velocity components along Z – axis under the effect of sudden disturbances.

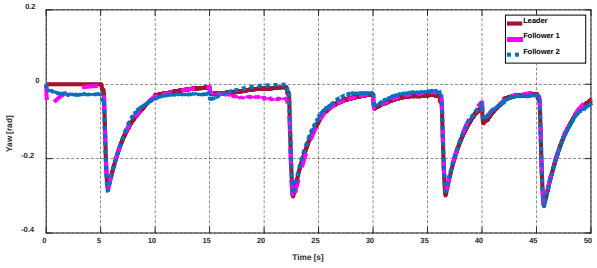

Figure 34. Yaw control for the cooperative quadrotors under the effect of sudden disturbances.

In order to validate the proposed controller, the controller introduced in this paper is compared with a backstepping-backstepping controller developed earlier for the same underlying system (Mahfouz et al., 2018). The trajectory of the leader quadrotor along the X-axis is shown in Figure 35 where both controllers under study succeeded to reject the effect of the applied sudden disturbances.

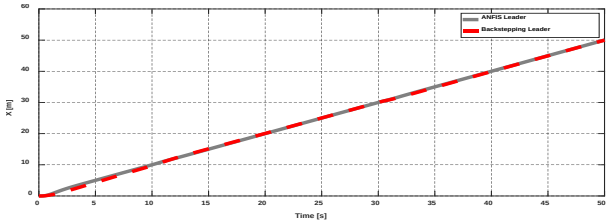

Figure 35. Path tracked by the leader quadrotor along the X –axis by ANFIS and backstepping under the effect of a disturbance.

Figure 36, and Figure 37 demonstrate the velocity and the pitch control of the leader in the presence of disturbances, respectively.

The ANFIS controller can reject the effect of the disturbance more than the backstepping controller.

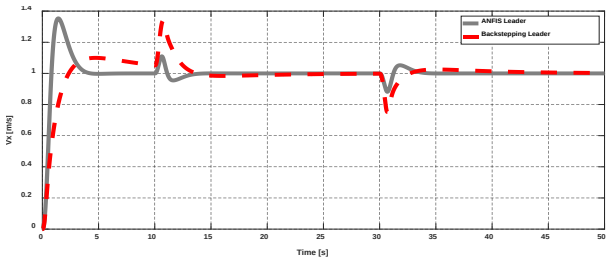

Figure 36. Velocity component of the leader along the X –axis by ANFIS and backstepping under the effect of a disturbance.

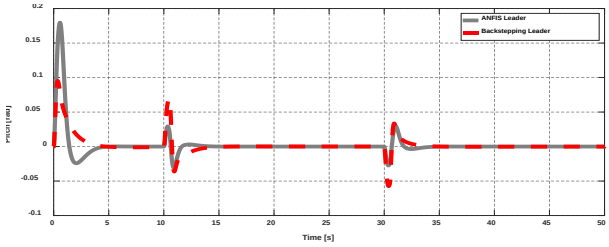

Figure 37. Pitch control for the leader quadrotor by ANFIS and backstepping controllers under the effect of a disturbance.

Similarly, Figure 38, Figure 39, and Figure 40 demonstrate the trajectory of the leader quadrotor along Y-axis, its velocity component and its roll control, respectively.

The results validate the success of the introduced hybrid control to reject the sudden disturbances over the backstepping controller.

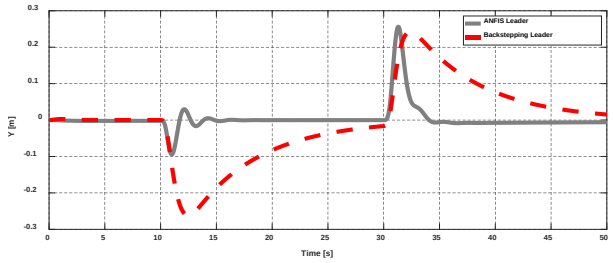

Figure 38. Path tracked by the leader quadrotor along Y -axis by ANFIS and backstepping under the effect of a disturbance.

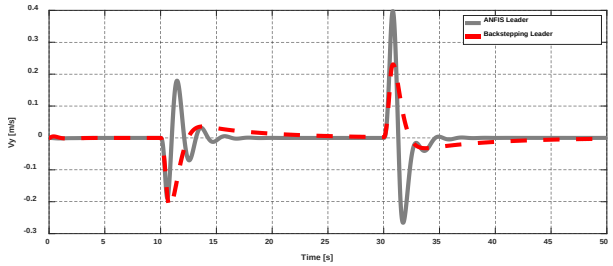

Figure 39. Velocity component of the leader along the Y –axis by ANFIS and backstepping under the effect of a disturbance.

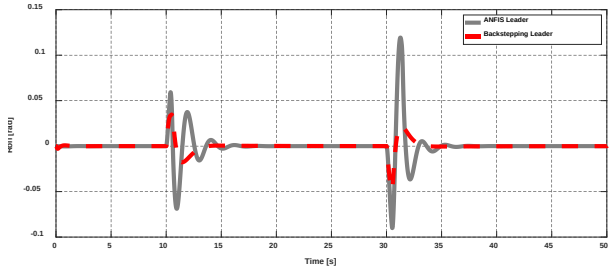

Figure 40. Roll control for the leader quadrotor by ANFIS and backstepping controllers under the effect of a disturbance.

Finally, Figure 41, Figure 42, and Figure 43 demonstrate the trajectory of the leader quadrotor along Z-axis, its velocity component and its yaw control, respectively. The results show the capacity of the ANFIS controller to dismiss the applied disturbances over the backstepping controller.

By investigating the results appear in the previously sketched figures, the proposed hybrid backstepping-ANFIS controller achieves good tracking of the reference in different scenarios. The comparison between the proposed hybrid controller and backstepping controller shows the superiority of the hybrid controller over the backstepping controller especially in stability analysis.

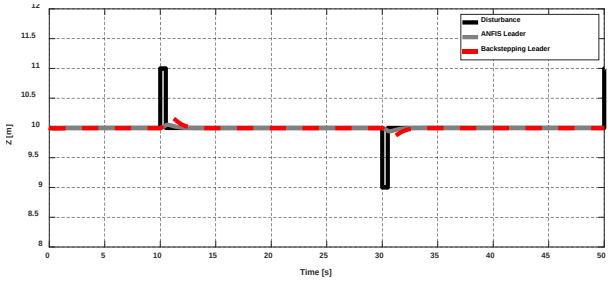

Figure 41. Path tracked by the leader quadrotor along Z -axis by ANFIS and backstepping under the effect of a disturbances.

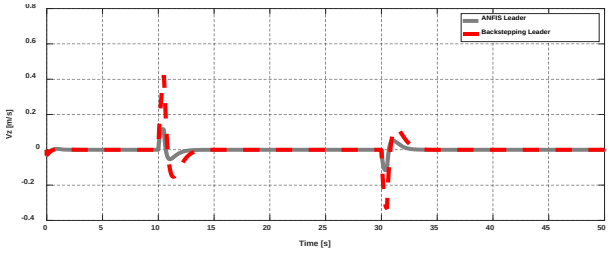

Figure 42. Velocity component along Z-axis position by ANFIS and backstepping controllers under the effect of disturbances.

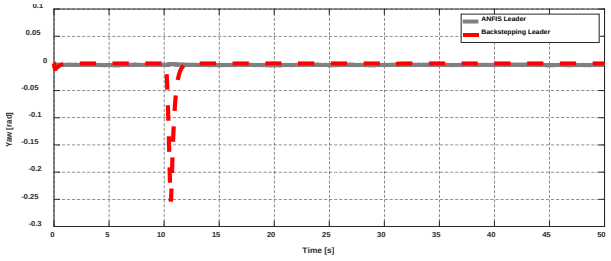

Figure 43. Yaw control for the leader quadrotor by ANFIS and backstepping controllers under the effect of disturbances.

6. Conclusion

In this paper, a cascaded backstepping and ANFIS controllers were designed as a robust hybrid controller for solving the formation problem for a group of cooperative quadrotors in free and loaded obstacle environment. The ANFIS controller was designed as a lower controller, while the backstepping controller is designed for the whole group as a higher controller. The outcomes acquired from the flight simulations show that the offered hybrid controller is fit for controlling a group of cooperative quadrotors for altitude and attitude set-points.

The yield information of the backstepping controlled framework is utilized as learning and checking information for

the ANFIS layout. The outcomes acquired utilizing ANFIS, as a nonlinear controller, are differentiated with the backstepping based-PID controller outcomes. The simulation outcomes show a stable flight is accomplished using the offered hybrid controller.

The stability of the controllers is observed at various points of operation by applying sudden disturbance pulses to the group members. The ANFIS controller as a low controller in the offered hybrid controller is superior to the backstepping controller.

The main contribution in this work lays in solving the formation problem for a team of cooperative quadrotors through hybrid backstepping and ANFIS controller in a free and loaded obstacle environment.

Future work will be applying the hybrid controller validated in this work on cooperative quadrotors in real time.

Conflict of interest

The authors have no conflict of interest to declare.

Acknowledgements

The authors would like to express their sincere gratitude to the faculty professors of MTC for their invaluable assistance and unwavering support. Their guidance and expertise have been instrumental in the successful completion of this work. Furthermore, the authors extend their heartfelt appreciation to TRC for granting them access to their state-of-the-art laboratories, which enabled them to carry out the necessary experiments and obtain accurate results. The authors recognize that this collaboration with MTC and TRC has been a truly enriching experience, and they are grateful for the opportunities it has provided.

Funding

The authors received no specific funding for this work.

References

Abbass, H. A. (2001). MBO: Marriage in honey bees optimization-A haplometrosis polygynous swarming approach. In *Proceedings of the 2001 congress on evolutionary computation (IEEE Cat. No. 01TH8546)* (Vol. 1, pp. 207-214). IEEE.
https://doi.org/10.1109/CEC.2001.934391

Al-Fetyani, M., Hayajneh, M., & Alsharkawi, A. (2021). Design of an executable anfis-based control system to improve the attitude and altitude performances of a quadcopter drone. *International Journal of Automation and Computing*, *18*, 124-140.
https://doi.org/10.1007/s11633-020-1251-2

Alfeo, A. L., Cimino, M. G., De Francesco, N., Lazzeri, A., Lega, M., & Vaglini, G. (2018). Swarm coordination of mini-UAVs for target search using imperfect sensors. *Intelligent Decision Technologies*, *12*(2), 149-162.
https://doi.org/10.3233/IDT-170317

Allahverdy, D., & Fakharian, A. (2019). A Back-Stepping Controller Scheme for Altitude Subsystem of Hypersonic Missile with ANFIS Algorithm. *Journal of Computer & Robotics*, *12*(1), 57-64.

Asad, Y. P., Shamsi, A., & Tavoosi, J. (2017). Backstepping-based recurrent type-2 fuzzy sliding mode control for MIMO systems (MEMS triaxial gyroscope case study). *International Journal of Uncertainty, Fuzziness and Knowledge-Based Systems*, *25*(02), 213-233.
https://doi.org/10.1142/S0218488517500088

Ashry, M. (2014). Comparative Study for Different Quad-Rotor Helicopter Feedback Controllers. *International Journal of Engineering Research and Technology*, *3*.

Ashry, M., Abou-Zayed, U., & Breikin, T. (2008). Control of multivariable systems using modified local optimal controller. *IFAC Proceedings Volumes*, *41*(2), 8767-8772.
https://doi.org/10.3182/20080706-5-KR-1001.01482

Ashry, M. M. (2019). Multivariable flight controller design for ultrastick-25e UAV. In *International Conference on Aerospace Sciences and Aviation Technology* (Vol. 18, No. 18, pp. 1-18). The Military Technical College.
10.1088/1757-899X/610/1/012014

Azar, A. T., Serrano, F. E., Flores, M. A., Vaidyanathan, S., & Zhu, Q. (2020). Adaptive neural-fuzzy and backstepping controller for port-Hamiltonian systems. *International Journal of Computer Applications in Technology*, *62(*1), 1-12. https://doi.org/10.1504/IJCAT.2020.103894

Azzam, A., & Wang, X. (2010). Quad rotor arial robot dynamic modeling and configuration stabilization. In *2010 2nd International Asia conference on informatics in control, automation and robotics (CAR 2010)* (Vol. 1, pp. 438-444). IEEE. https://doi.org/10.1109/CAR.2010.5456804

Bang, H., Lee, J.-S., & Eun, Y.-J. (2004). Nonlinear attitude control for a rigid spacecraft by feedback linearization. *Journal of Mechanical Science and Technology*, *18*(2), 203-210. https://doi.org/10.1007/BF03184729

Basri, M. A. M., Husain, A. R., & Danapalasingam, K. A. (2015). Nonlinear Control of an Autonomous Quadrotor Unmanned Aerial Vehicle using Backstepping Controller Optimized by Particle Swarm Optimization. *Journal of Engineering Science & Technology Review*, *8*(3). https://doi.org/10.25103/jestr.083.05

Bouabdallah, S. (2007). *Design and control of quadrotors with application to autonomous flying* (No. THESIS). Epfl. https://doi.org/10.5075/epfl-thesis-3727

Bouabdallah, S., & Siegwart, R. (2007). Full control of a quadrotor. In *2007 IEEE/RSJ international conference on intelligent robots and systems* (pp. 153-158). Ieee. https://doi.org/10.1109/IROS.2007.4399042

Colorni, A., Dorigo, M., & Maniezzo, V. (1991). Distributed optimization by ant colonies. In *Proceedings of the first European conference on artificial life* (Vol. 142, pp. 134-142).

Eberhart, R., & Kennedy, J. (1995). A new optimizer using particle swarm theory. In *MHS'95. Proceedings of the sixth international symposium on micro machine and human science* (pp. 39-43). IEEE. https://doi.org/10.1109/MHS.1995.494215

Ekawati, E., Budi, E. M., Mukhlish, F., Putra, N. M., & Prasetyo, R. (2016). The development of swarm control on quadrotor with visual localization and proportional-integral velocity controller. In *2016 International Conference on Instrumentation, Control and Automation (ICA)* (pp. 6-11). IEEE. https://doi.org/10.1109/ICA.2016.7811466

Elloumi, M., Dhaou, R., Escrig, B., Idoudi, H., & Saidane, L. A. (2018, April). Monitoring road traffic with a UAV-based system. In *2018 IEEE wireless communications and networking conference (WCNC)* (pp. 1-6). IEEE. https://doi.org/10.1109/WCNC.2018.8377077

Eusuff, M. M., & Lansey, K. E. (2003). Optimization of water distribution network design using the shuffled frog leaping algorithm. *Journal of Water Resources planning and management*, *129*(3), 210-225.

Farinelli, A., Iocchi, L., & Nardi, D. (2004). Multirobot systems: a classification focused on coordination. *IEEE Transactions on Systems, Man, and Cybernetics*, Part B (Cybernetics), 34(5), 2015-2028. https://doi.org/10.1109/TSMCB.2004.832155

Ferdaus, M. M., Pratama, M., Anavatti, S. G., Garratt, M. A., & Lughofer, E. (2018). PAC: A novel self-adaptive neuro-fuzzy controller for micro aerial vehicles. *Information sciences*, *512*, 481-505. https://doi.org/10.48550/arXiv.1811.03764

Fethalla, N., Saad, M., Michalska, H., & Ghommam, J. (2017). Robust observer-based backstepping controller for a quadrotor UAV. In *2017 IEEE 30th Canadian Conference on Electrical and Computer Engineering (CCECE)* (pp. 1-4). IEEE. https://doi.org/10.1109/CCECE.2017.7946754

Fichera, F. (2013). *Lyapunov techniques for a class of hybrid systems and reset controller syntheses for continuous-time plants* (Doctoral dissertation, ISAE-TOULOUSE). https://theses.hal.science/tel-00919930/

Finn, R. L., & Wright, D. (2012). Unmanned aircraft systems: Surveillance, ethics and privacy in civil applications. *Computer Law & Security Review*, *28*(2), 184-194. https://doi.org/10.1016/j.clsr.2012.01.005

Gallay, M., Eck, C., Zgraggen, C., Kaňuk, J., & Dvorný, E. (2016). High resolution airborne laser scanning and hyperspectral imaging with a small UAV platform. *The International Archives of Photogrammetry, Remote Sensing and Spatial Information Sciences*, *41*, 823.

Gharibi, M., Boutaba, R., & Waslander, S. L. (2016). Internet of Drones. *IEEE Access, 4*, 1148-1162. https://doi.org/10.1109/access.2016.2537208

Greatwood, C., Richardson, T., Freer, J., Thomas, R., MacKenzie, A., Brownlow, R., Lowry, D., Fisher, R., & Nisbet, E. (2017). Atmospheric sampling on ascension island using multirotor UAVs. *Sensors*, *17*(6), 1189. https://doi.org/10.3390/s17061189

Gupte, S., Mohandas, P. I. T., & Conrad, J. M. (2012). A survey of quadrotor unmanned aerial vehicles. *2012 Proceedings of IEEE Southeastcon*, 1-6. https://doi.org/10.1109/SECon.2012.6196930

Hamel, T., Mahony, R., Lozano, R., & Ostrowski, J. (2002). Dynamic modelling and configuration stabilization for an X4-flyer. *IFAC Proceedings Volumes*, *35*(1), 217-222. https://doi.org/10.3182/20020721-6-ES-1901.00848

Hou, Z., Wang, W., Zhang, G., & Han, C. (2017). A survey on the formation control of multiple quadrotors. In *2017 14th International Conference on Ubiquitous Robots and Ambient Intelligence (URAI)* (pp. 219-225). IEEE. https://doi.org/10.1109/URAI.2017.7992717

Jang, J. S. (1993). ANFIS: adaptive-network-based fuzzy inference system. IEEE transactions on systems, man, and cybernetics, *23*(3), 665-685. https://doi.org/10.1109/21.256541

Jia, Z., Wan, Y. H., Zhou, Y. J., Jiang, G. P., & Zhang, D. (2018). Formation shape control of multi-UAV with collision avoidance. In *2018 33rd Youth Academic Annual Conference of Chinese Association of Automation (YAC)* (pp. 305-310). IEEE. https://doi.org/10.1109/YAC.2018.8406390

Karaboga, D. (2005). *An idea based on honey bee swarm for numerical optimization* (Vol. 200, pp. 1-10). Technical report-tr06, Erciyes university, engineering faculty, computer engineering department.

Karaboga, D., & Kaya, E. (2019). Adaptive network based fuzzy inference system (ANFIS) training approaches: a comprehensive survey. *Artificial Intelligence Review*, *52*, 2263-2293. https://doi.org/10.1007/s10462-017-9610-2

Khari, S., Rahmani Cherati, Z., Rezaie, B., & Sadati, S. J. (2015). Chaos control based on combination of Integral Terminal Sliding Mode with a new sliding surface and adaptive neuro-fuzzy inference system. *Journal of control*, *9*(3), 37-50.

Kıvrak, A. Ö. (2006). *Design of Control Systems for a Quadrotor Flight Vehicle Equipped with Internal Sensors*. Atılım Üniversitesi.

Kumari, N., & Sunita, S. (2013). Comparison of ANNs, fuzzy logic and neuro-fuzzy integrated approach for diagnosis of coronary heart disease: a survey. *International Journal of Computer Science and Mobile Computing*, *2*(6), 216-224.

Lee, K. U., Choi, Y. H., & Park, J. B. (2017). Backstepping Based Formation Control of Quadrotors with the State Transformation Technique. *Applied Sciences*, *7*(11), 1170. https://doi.org/10.3390/app7111170

Li, L., Sun, L., & Jin, J. (2015). Survey of advances in control algorithms of quadrotor unmanned aerial vehicle. In *2015 IEEE 16th international conference on communication technology (ICCT)* (pp. 107-111). IEEE. https://doi.org/10.1109/ICCT.2015.7399803

Li, Z., Liu, Y., Hayward, R., Zhang, J., & Cai, J. (2008). Knowledge-based power line detection for UAV surveillance and inspection systems. In *2008 23rd International Conference Image and Vision Computing New Zealand* (pp. 1-6). IEEE. https://doi.org/10.1109/IVCNZ.2008.4762118

Liu, H., Wang, X., & Zhu, H. (2015). A novel backstepping method for the three-dimensional multi-UAVs formation control. In *2015 IEEE International Conference on Mechatronics and Automation (ICMA)* (pp. 923-928). IEEE. https://doi.org/10.1109/ICMA.2015.7237609

Liu, T., Li, R., Zhong, X., Jiang, M., Jin, X., Zhou, P., Liu, S., Sun, C., & Guo, W. (2018). Estimates of rice lodging using indices derived from UAV visible and thermal infrared images. *Agricultural and forest meteorology*, 252, 144-154. https://doi.org/10.1016/j.agrformet.2018.01.021

Liu, X., & Zhou, Z. (2017). A novel prediction model based on particle swarm optimization and adaptive neuro-fuzzy inference system. *Journal of Intelligent & Fuzzy Systems*, *33*(5), 3137-3143. https://doi.org/10.3233/JIFS-169365

Madani, T., & Benallegue, A. (2006). Backstepping control for a quadrotor helicopter. In *2006 IEEE/RSJ International Conference on Intelligent Robots and Systems* (pp. 3255-3260). IEEE. https://doi.org/10.1109/IROS.2006.282433

Mahfouz, M., Ashry, M., & Elnashar, G. (2013). Design and control of quad-rotor helicopters based on adaptive neuro-fuzzy inference system. *International Journal of Engineering Research and Technology*, *2*(12), 479-485.

Mahfouz, M., Hafez, A. T., Ashry, M., & Elnashar, G. (2018). Formation configuration for cooperative multiple UAV via backstepping PID controller. In *2018 AIAA SPACE and Astronautics Forum and Exposition* (p. 5282).
https://doi.org/10.2514/6.2018-5282

Mahfouz, M., Hafez, A. T., Ashry, M. M., & Elnashar, G. (2020). Formation Reconfiguration Based on Backstepping-PID Controller for Collaborative Quadrotors. In *2020 12th International Conference on Electrical Engineering (ICEENG)* (pp. 396-401). IEEE.
https://doi.org/10.1109/ICEENG45378.2020.9171779

Mahfouz, M., Hafez, A. T., Azzam, A., Ashry, M. M., & Elnashar, G. (2020). Formation Reconfiguration in Dynamic Obstacle Loaded Environment via Backstepping Approach. 2020 12th International Conference on Electrical Engineering (ICEENG),
https://doi.org/10.1109/ICEENG45378.2020.9171727

Mahfouz, M., Taiomour, A., Ashry, M. M., & Elnashar, G. (2019). PID vs. Backstepping Control for Cooperative Quadrotors Unmanned Aerial Vehicles. In *IOP Conference Series: Materials Science and Engineering* (Vol. 610, No. 1, p. 012057). IOP Publishing.
https://doi.org/10.1088/1757-899X/610/1/012057

Mahjri, I., Dhraief, A., & Belghith, A. (2015). A review on collision avoidance systems for unmanned aerial vehicles. In *Communication Technologies for Vehicles: 8th International Workshop, Nets4Cars/Nets4Trains/Nets4Aircraft 2015, Sousse, Tunisia, May 6-8, 2015. Proceedings 8* (pp. 203-214). Springer International Publishing.
https://doi.org/10.1007/978-3-319-17765-6_18

Martinez Martinez, V. (2007). Modelling of the flight dynamics of a quadrotor helicopter.

Mori, T., Hashimoto, T., Terada, A., Yoshimoto, M., Kazahaya, R., Shinohara, H., & Tanaka, R. (2016). Volcanic plume measurements using a UAV for the 2014 M*t. Ontake eruption. Earth, Planets and Space*, *68*(1), 49.
https://doi.org/10.1186/s40623-016-0418-0

Murray, R. M., Li, Z., Sastry, S. S., & Sastry, S. S. (1994). A mathematical introduction to robotic manipulation. *CRC press*.
https://doi.org/10.1201/9781315136370

Muslimi, B., Capretz, M. A., & Samarabandu, J. (2006). An efficient technique for extracting fuzzy rules from neural networks. *International Journal of Intelligent Technology*, *1*(4), 299-305.

Mutawe, S., Hayajneh, M., & BaniHani, S. (2021). Robust Path Following Controllers for Quadrotor and Ground Robot. In *2021 International Conference on Electrical, Communication, and Computer Engineering (ICECCE)* (pp. 1-6). IEEE.
https://doi.org/10.1109/ICECCE52056.2021.9514140

Nakano, T., Kamiya, I., Tobita, M., Iwahashi, J., & Nakajima, H. (2014). Landform monitoring in active volcano by UAV and SFM-MVS technique. *The International Archives of Photogrammetry, Remote Sensing and Spatial Information Sciences*, *40*(8), 71.
https://doi.org/10.5194/isprsarchives-XL-8-71-2014

Navarro, R. I., & Akhi-Elarab, F. N. (2013). Study of a neural network-based system for stability augmentation of an airplane.
MSc thesis, Universitat Politecnica de Catalunya, Spain (accessed 20 September 2013)].

Ghazbi, S. N., Aghli, Y., Alimohammadi, M., & Akbari, A. A. (2016). Quadrotors unmanned aerial vehicles: A review. *International journal on smart sensing and Intelligent Systems*, *9*(1), 309-333.
https://doi.org/10.21307/ijssis-2017-872

Oh, H., Shirazi, A. R., Sun, C., & Jin, Y. (2017). Bio-inspired self-organising multi-robot pattern formation: A review. *Robotics and Autonomous Systems*, *91*, 83-100.
https://doi.org/10.1016/j.robot.2016.12.006

Okubo, A. (1986). Dynamical aspects of animal grouping: swarms, schools, flocks, and herds. *Advances in biophysics*, *22*, 1-94.
https://doi.org/10.1016/0065-227X(86)90003-1

Özbek, N. S., Önkol, M., & Efe, M. Ö. (2015). Feedback control strategies for quadrotor-type aerial robots: a survey. *Transactions of the Institute of Measurement and Control*, *38*(5), 529-554.
https://doi.org/10.1177/0142331215608427

Parrish, J. K., Viscido, S. V., & Grunbaum, D. (2002). Self-organized fish schools: an examination of emergent properties. *The biological bulletin*, *202*(3), 296-305.

Premkumar, K., & Manikandan, B. (2018). Stability and Performance Analysis of ANFIS Tuned PID Based Speed Controller for Brushless DC Motor. *Current Signal Transduction Therapy*, *13*(1), 19-30.
https://doi.org/10.2174/1574362413666180226105809

Rahman, M. F. A., Ani, A. I. C., Yahaya, S. Z., Hussain, Z., Boudville, R., & Ahmad, A. (2016). Implementation of quadcopter as a teaching tool to enhance engineering courses. In *2016 IEEE 8th International Conference on engineering education (ICEED)* (pp. 32-37). IEEE. https://doi.org/10.1109/ICEED.2016.7856089

Raymer, D. (2012). *Aircraft design: a conceptual approach*. American Institute of Aeronautics and Astronautics, Inc.. https://doi.org/10.2514/4.869112

Rego, B. S., Adorno, B. V., & Raffo, G. V. (2016, October). Formation backstepping control based on the cooperative dual task-space framework: a case study on unmanned aerial vehicles. In *2016 XIII Latin American Robotics Symposium and IV Brazilian Robotics Symposium (LARS/SBR)* (pp. 163-168). IEEE. https://doi.org/10.1109/LARS-SBR.2016.34

Reynolds, C. W. (1987). Flocks, herds and schools: A distributed behavioral model. In *Proceedings of the 14th annual conference on Computer graphics and interactive techniques* (pp. 25-34). https://doi.org/10.1145/37401.37406

Ryan, J. C., Hubbard, A., Box, J. E., Brough, S., Cameron, K., Cook, J. M., Cooper, M., Doyle, S. H., Edwards, A., & Holt, T. (2017). Derivation of high spatial resolution albedo from UAV digital imagery: application over the Greenland Ice Sheet. *Frontiers in Earth Science*, *5,* 40. https://doi.org/10.3389/feart.2017.00040

Shakernia, O., Ma, Y., Koo, T. J., & Sastry, S. (1999). Landing an unmanned air vehicle: Vision based motion estimation and nonlinear control. *Asian journal of control*, *1*(3), 128-145. https://doi.org/10.1111/j.1934-6093.1999.tb00014.x

Shakhatreh, H., Sawalmeh, A. H., Al-Fuqaha, A., Dou, Z., Almaita, E., Khalil, I., ... & Guizani, M. (2019). Unmanned aerial vehicles (UAVs): A survey on civil applications and key research challenges. *Ieee Access*, *7*, 48572-48634. https://ieeexplore.ieee.org/abstract/document/8682048

Shinners, S. M. (1998). Modern control system theory and design. John Wiley & Sons.

Sun, Y., Huang, Z., & Chen, Y. (2014). ELA: a new swarm intelligence algorithm. In *2014 IEEE International Conference on Progress in Informatics and Computing* (pp. 109-113). IEEE. https://doi.org/10.1109/PIC.2014.6972306

Tavoosi, J. (2020). Sliding mode control of a class of nonlinear systems based on recurrent type-2 fuzzy RBFN. *International Journal of Mechatronics and Automation*, *7*(2), 72-80. https://doi.org/10.1504/IJMA.2020.108797

Tayebi, A., & McGilvray, S. (2006). Attitude stabilization of a VTOL quadrotor aircraft. *IEEE Transactions on control systems technology*, *14*(3), 562-571. https://doi.org/10.1109/TCST.2006.872519

Techy, L., Schmale III, D. G., & Woolsey, C. A. (2010). Coordinated aerobiological sampling of a plant pathogen in the lower atmosphere using two autonomous unmanned aerial vehicles. *Journal of Field Robotics, 27(*3), 335-343. https://doi.org/10.1002/rob.20335

Totoki, Y., Suemitsu, H., & Matsuo, T. (2009). Decay rate estimation of continuous time series using instantaneous Lyapunov exponent. In *2009 ICCAS-SICE* (pp. 5073-5077). IEEE. https://ieeexplore.ieee.org/abstract/document/5334492

Vallejo-Alarcón, M., Castro-Linares, R., & Velasco-Villa, M. (2015). Unicycle-type robot & quadrotor leader-follower formation backstepping control. *IFAC-PapersOnLine*, *48*(19), 51-56. https://doi.org/10.1016/j.ifacol.2015.12.009

Werbos, P. J. (1992). Neurocontrol and fuzzy logic: connections and designs. *International Journal of Approximate Reasoning*, *6*(2), 185-219. https://doi.org/10.1016/0888-613X(92)90017-T

Wierema, M. (2008). Design, implementation and flight test of indoor navigation and control system for a quadrotor UAV. *Master of Science in Aerospace Engineering at Delft University of Technology.*

Wu, F., Chen, J., & Liang, Y. (2017). Leader-follower formation control for quadrotors. In *IOP conference series: materials science and engineering* (Vol. 187, No. 1, p. 012016). IOP Publishing. https://doi.org/10.1088/1757-899X/187/1/012016

Wu, H. S., Zhang, F., & Wu, L. (2013). New swarm intelligence algorithm-wolf pack algorithm. *Systems engineering and electronics*, *35*(11), 2430-2438.

Wu, Y. (2009). Development and Implementation of a Control System for a Quadrotor UAV. *Hochschule Ravensburg-Weingarten.*

Yang, F., Ji, X., Yang, C., Li, J., & Li, B. (2017). Cooperative search of UAV swarm based on improved ant colony algorithm in uncertain environment. In *2017 IEEE International Conference on Unmanned Systems (ICUS)* (pp. 231-236). Ieee.
https://doi.org/10.1109/ICUS.2017.8278346

Yang, F., Wang, P., Zhang, Y., Zheng, L., & Lu, J. (2017). Survey of swarm intelligence optimization algorithms. In *2017 IEEE International Conference on Unmanned Systems (ICUS)* (pp. 544-549). IEEE.
https://doi.org/10.1109/ICUS.2017.8278405

Yang, X. S. (2010a). Nature-inspired metaheuristic algorithms. Luniver press.

Yang, X. S. (2010b). A new metaheuristic bat-inspired algorithm. In *Nature inspired cooperative strategies for optimization (NICSO 2010)* (pp. 65-74). Berlin, Heidelberg: Springer Berlin Heidelberg.
https://doi.org/10.1007/978-3-642-12538-6_6

Yang, X. S. (2012). Flower pollination algorithm for global optimization. In *International conference on unconventional computing and natural computation* (pp. 240-249). Berlin, Heidelberg: Springer Berlin Heidelberg.
https://doi.org/10.1007/978-3-642-32894-7

Yang, X. S., & Deb, S. (2009). Cuckoo Search via Lévy flights. In *2009 World Congress on Nature & Biologically Inspired Computing (NaBIC)* (p. 210). IEEE.
https://doi.org/10.1109/NABIC.2009.5393690

Yong, S. P., & Tuan, L. T. (2006). A Fuzzy Neural Based Data Classification System. In *Conference on Data Mining (DMIN 2006)*.

Zhang, X., Li, X., Wang, K., & Lu, Y. (2014). A Survey of Modelling and Identification of Quadrotor Robot. *Abstract and Applied Analysis*, 2014, 16.
https://doi.org/10.1155/2014/320526

Zhang, Y., & Mehrjerdi, H. (2013, May). A survey on multiple unmanned vehicles formation control and coordination: Normal and fault situations. In *2013 International conference on unmanned aircraft systems (ICUAS)* (pp. 1087-1096). IEEE.
https://doi.org/10.1109/ICUAS.2013.6564798

Zhu, B., Xie, L., & Han, D. (2016). Recent developments in control and optimization of swarm systems: A brief survey. In *2016 12th IEEE international conference on control and automation (ICCA)* (pp. 19-24). IEEE.
https://doi.org/10.1109/ICCA.2016.7505246

Zulu, A., & John, S. (2016). A review of control algorithms for autonomous quadrotors.
https://doi.org/10.4236/ojapps.2014.414053